haematologica
Journal of The Ferrata Storti Foundation

KMT2D mutations and *TP53* disruptions are poor prognostic biomarkers in mantle cell lymphoma receiving high-dose therapy: a FIL study

by Simone Ferrero, Davide Rossi, Andrea Rinaldi, Alessio Bruscaggin, Valeria Spina, Christian W. Eskelund, Andrea Evangelista, Riccardo Moia, Ivo Kwee, Christina Dahl, Alice Di Rocco, Vittorio Stefoni, Fary Diop, Chiara Favini, Paola Ghione, Abdurraouf Mokhtar Mahmoud, Mattia Schipani, Arne Kolstad, Daniela Barbero, Domenico Novero, Marco Paulli, Alberto Zamò, Mats Jerkeman, Maria Gomez da Silva, Armando Santoro, Annalia Molinari, Andres Ferreri, Kirsten Grønbæk, Andrea Piccin, Sergio Cortelazzo, Francesco Bertoni, Marco Ladetto, and Gianluca Gaidano

Haematologica 2019 [Epub ahead of print]

Citation: Simone Ferrero, Davide Rossi, Andrea Rinaldi, Alessio Bruscaggin, Valeria Spina, Christian W. Eskelund, Andrea Evangelista, Riccardo Moia, Ivo Kwee, Christina Dahl, Alice Di Rocco, Vittorio Stefoni, Fary Diop, Chiara Favini, Paola Ghione, Abdurraouf Mokhtar Mahmoud, Mattia Schipani, Arne Kolstad, Daniela Barbero, Domenico Novero, Marco Paulli, Alberto Zamò, Mats Jerkeman, Maria Gomez da Silva, Armando Santoro, Annalia Molinari, Andres Ferreri, Kirsten Grønbæk, Andrea Piccin, Sergio Cortelazzo, Francesco Bertoni, Marco Ladetto, and Gianluca Gaidano. KMT2D mutations and TP53 disruptions are poor prognostic biomarkers in mantle cell lymphoma receiving high-dose therapy: a FIL study.
Haematologica. 2019; 104:xxx
doi:10.3324/haematol.2018.214056

KMT2D **mutations and** ***TP53*** **disruptions are poor prognostic biomarkers in mantle cell lymphoma receiving high-dose therapy: a FIL study**

Simone Ferrero[1,2], Davide Rossi*[3,4], Andrea Rinaldi*[4], Alessio Bruscaggin[4], Valeria Spina[4], Christian W Eskelund[5,6], Andrea Evangelista[7], Riccardo Moia[8], Ivo Kwee[4,9,10], Christina Dahl[11], Alice Di Rocco[12], Vittorio Stefoni[13], Fary Diop[8], Chiara Favini[8], Paola Ghione[1], Abdurraouf Mokhtar Mahmoud[8], Mattia Schipani[8], Arne Kolstad[14], Daniela Barbero[1], Domenico Novero[15], Marco Paulli[16], Alberto Zamò[17,18], Mats Jerkeman[19], Maria Gomes da Silva[20], Armando Santoro[21], Annalia Molinari[22], Andres Ferreri[23], Kirsten Grønbæk[5,6], Andrea Piccin[24], Sergio Cortelazzo[25], Francesco Bertoni°[4], Marco Ladetto°[26] and Gianluca Gaidano°[8]*

[1]Department of Molecular Biotechnologies and Health Sciences - Hematology Division, Università di Torino, Torino, Italy; [2]Hematology Division, AOU Città della Salute e della Scienza di Torino, Torino, Italy; [3]Hematology, Oncology Institute of Southern Switzerland, Bellinzona, Switzerland; [4]Universita' della Svizzera italiana, Institute of Oncology Research, Bellinzona, Switzerland; [5]Department of Hematology, Rigshospitalet, Copenhagen, Denmark; [6]Biotech Research and Innovation Centre, Copenhagen, Denmark; [7]Clinical Epidemiology, Città della Salute e della Scienza and CPO Piemonte, Torino, Italy; [8]Division of Hematology, Department of Translational Medicine, University of Eastern Piedmont, Novara, Italy; [9]Swiss Institute of Bioinformatics (SIB), Lausanne, Switzerland; [10]Dalle Molle Institute for Artificial Intelligence (IDSIA), Manno, Switzerland; [11]Danish Cancer Society Research Center, Copenhagen, Denmark; [12]Department of Cellular Biotechnologies and Hematology, Policlinico Umberto I, "Sapienza" University of Rome, Roma, Italy; [13]Institute of Hematology "L. e A. Seràgnoli", University of Bologna, Bologna, Italy; [14]Department of Oncology, Oslo University Hospital, Oslo, Norway; [15]First unit of Pathology, AOU Città della Salute e della Scienza di Torino,

Torino, Italy; [16]Unit of Anatomic Pathology, Department of Molecular Medicine, Fondazione IRCCS Policlinico San Matteo and Università degli Studi di Pavia, Pavia, Italy; [17]Department of Oncology, Università di Torino, Torino, Italy; [18]Department of Diagnostics and Public Health, University of Verona, Italy; [19]Department of Oncology, Lund University Hospital, Lund, Sweden; [20]Department of Hematology, Instituto Português de Oncologia de Lisboa, Lisboa, Portugal; [21]Humanitas Cancer Center, Humanitas Clinical and Research Center, Rozzano, Italy; [22]Hematology, Ospedale degli Infermi, Rimini, Italy; [23]Lymphoma Unit, Department of Onco-Haematology, IRCCS San Raffaele Scientific Institute, Milano, Italy; [24]Department of Hematology, Ospedale Generale, Bolzano, Italy; [25]Oncology Unit, Humanitas/Gavazzeni Clinic, Bergamo, Italy; [26]SC Ematologia, Azienda Ospedaliera Santi Antonio e Biagio e Cesare Arrigo, Alessandria, Italy.

* These Authors equally contributed as First Authors

° These Authors equally contributed as Senior Authors

Corresponding author:

Simone Ferrero, MD

Department of Molecular Biotechnologies and Health Sciences - Hematology Division, University of Torino/AOU “Città della Salute e della Scienza di Torino”, Torino, Italy

Phone: +390116334220-6884

Fax: +390116963737

E-mail: simone.ferrero@unito.it

Running title: *KMT2D* mutations and *TP53* disruptions in MCL

DISCLOSURES: DR: Honoraria (Abbvie, Gilead, Janssen, Roche), Research Grant (Abbvie, Gilead) All the other Authors have no conflict of interests to declare.

ACKNOWLEDGEMENTS

This work was supported by: Progetto di Rilevante Interesse Nazionale (PRIN2009) from Ministero Italiano dell'Università e della Ricerca (MIUR), Roma, Italy [7.07.02.60 AE01]; Progetto di Ricerca Sanitaria Finalizzata 2009 [RF-2009-1469205] and 2010 [RF-2010-2307262 to S.C.], A.O.S. Maurizio, Bolzano/Bozen, Italy; Fondi di Ricerca Locale, Università degli Studi di Torino, Italy; Fondazione Neoplasie Del Sangue (Fo.Ne.Sa), Torino, Italy; Fondazione CRT (project codes: 2016.0677 and 2018.1284), Torino, Italy; Associazione DaRosa, Torino, Italy; Molecular bases of disease dissemination in lymphoid malignancies to optimize curative therapeutic strategies, (5 x 1000 No. 21198), Associazione Italiana per la Ricerca sul Cancro Foundation Milan, Italy; Progetto Ricerca Finalizzata RF-2011-02349712, Ministero della Salute, Rome, Italy; and PRIN 2015ZMRFEA_004, MIUR, Rome, Italy; Partially funded by the AGING Project – Department of Excellence – DIMET, Università del Piemonte Orientale, Novara, Italy; Grant No. KFS-3746-08-2015, Swiss Cancer League, Bern, Switzerland; Grant No. KLS-3636-02-2015, Swiss Cancer League, Bern, Switzerland; Grant No. 320030_169670/1 Swiss National Science Foundation, Berne, Switzerland; iCARE No. 17860, Associazione Italiana per la Ricerca sul Cancro and Unione Europea, Milan, Italy; Fondazione Fidinam, Lugano, Switzerland; Nelia & Amadeo Barletta Foundation, Lausanne, Switzerland; Fondazione Ticinese per la Ricerca sul Cancro, Bellinzona, Switzerland; Novara-AIL Onlus, Novara, Italy.

Authors contribution

DR, SC, FB, ML and GG designed and performed research; SF, DR, ADR, ViSt, PG, MGdS, AS, AM, AF, AP, SC, ML and GG enrolled patients; SF, DB, DN, MP, ML and AZ provided biological samples SF, DR, AR, AB, VaSp, IK, FD, CF and DB performed research; SF, DR, AR, AB, VaSp, AE, RM and IK analysed data; CWE, CD, AK, MJ and KG provided data for the validation; SF, DR, AE, RM, FB, ML and GG wrote the paper.

The authors would like to thank all the patients who participated in the study. We are grateful to Gian Maria Zaccaria[1], Marco Ghislieri[1], Paola Ghione[1] and Andrea Piccin (Department of Hematology, Ospedale Generale, Bolzano, Italy) for their scientific advice and to Luigia Monitillo[1], Antonella Fiorillo[1], Antonella Ferranti[25] and Daniela Gioia[25] for their assistance.

ABSTRACT

In recent years, the outcome of mantle cell lymphoma has improved, especially in younger patients, receiving cytarabine-containing chemoimmunotherapy and autologous stem cell transplantation. Nevertheless, a proportion of mantle cell lymphoma patients still experience early failure. To identify biomarkers anticipating failure of intensive chemotherapy in mantle cell lymphoma, we performed target resequencing and DNA profiling of purified tumor samples collected from patients enrolled in the prospective FIL-MCL0208 phase III trial (high-dose chemoimmunotherapy followed by autologous transplantation and randomized lenalidomide maintenance). Mutations of *KMT2D* and disruption of *TP53* by deletion or mutation associated with an increased risk of progression and death, both in univariate and multivariate analysis. By adding *KMT2D* mutations and *TP53* disruption to the MIPI-c backbone, we derived a new prognostic index, the "MIPI-genetic". The "MIPI-g" improved the model discrimination ability compared to the MIPI-c alone, defining three risk groups: *i)* low-risk patients (4-years progression free survival and overall survival of 72.0% and 94.5%); *ii)* intermediate-risk patients (4-years progression free survival and overall survival of 42.2% and 65.8%) and *iii)* high-risk patients (4-years progression free survival and overall survival of 11.5% and 44.9%). Our results: *i)* confirm that *TP53* disruption identifies a high-risk population characterized by poor sensitivity to conventional or intensified chemotherapy; *ii)* provide the pivotal evidence that patients harboring *KMT2D* mutations share the same poor outcome as patients harboring *TP53* disruption; and *iii)* allow to develop a tool for the identification of high-risk mantle cell lymphoma patients for whom novel therapeutic strategies need to be investigated. (Trial registered at clinicaltrials.gov identifier: NCT02354313)

INTRODUCTION

The introduction of high dose cytarabine-containing chemoimmunotherapeutic regimens and autologous transplantation (ASCT) have considerably improved the outcome of young fit mantle cell lymphoma (MCL) patients. Nonetheless, approximately 20 to 25% of MCL patients demonstrate inadequate efficacy of intensified chemoimmunotherapy as they are either primary refractory or relapse within two years from autologous stem cell transplantation.[1-5]

Clinical and pathological scores, including the MCL international prognostic index (MIPI),[6] the Ki-67 proliferative index,[7] and their combination in the MIPI-c score, stratify MCL patients in groups at different risk of relapse.[8] However, none of these tools has sufficient positive predictive value to trigger the development of tailored schedules specifically designed for high risk patients.[9]

Several recurrent mutations have been described in MCL, affecting DNA repair genes and cell cycle regulators (*TP53*, *ATM*, *CCND1*), epigenetic regulation genes (*KMT2D*, *WHSC1*) and cell-signaling pathways genes (*NOTCH1-2, BIRC3*, *TRAF2*).[10-12] The proof of principle that MCL genetics can impact on disease outcome stems from studies that have focused on the *TP53* tumor suppressor gene, including both mutations and 17p deletions.[13-17]

We prospectively assessed the clinical impact of a panel of genomic alterations in a cohort of young MCL patients treated with high dose chemoimmunotherapy and ASCT from the Fondazione Italiana Linfomi (FIL) "MCL0208" phase III trial.[18] The results document that *KMT2D* mutations associate with poor outcome in MCL and, along with *TP53* mutations and 17p deletions, might be integrated in a new prognostic score to segregate a subgroup of patients who obtain minimal or no benefit from intensive chemoimmunotherapy. The prognostic score was validated in an independent series of cases.

METHODS

Patients series

The FIL-MCL0208 (NCT02354313) is a phase III, multicenter, open-label, randomized, controlled study, designed to determine the efficacy of lenalidomide as maintenance versus observation in young (18-65 years old), fit, advanced stage (Ann arbor II-IV) MCL patients after first line intensified and high-dose chemo-immunotherapy followed by ASCT. Cases of non-nodal MCL were excluded.[19] The clinical trial, as well as the ancillary mutational study, were approved by the Ethical Committees of all the enrolling Centers. All patients provided written informed consent for the use of their biological samples for research purposes, in accordance with Institutional Review Boards requirements and the Helsinki's declaration. Clinical results of the fist interim analysis of the trial were already presented.[18] Further information are supplied in the Supplementary appendix.

Biological samples

Tumor cells were sorted from the baseline BM samples by immunomagnetic beads (CD19 MicroBeads,human-Miltenyi Biotec GmbH, Bergisch Gladbach, Germany) and stocked as dry pellets. Tumor DNA was extracted according to DNAzol protocol (Life Technologies). Germline DNA was obtained from PB mononuclear cells collected under treatment and proven to be tumor free by MRD analysis. Further information are supplied in the Supplementary appendix.

Next generation sequencing

A targeted resequencing panel (target region: 37’821 bp) (Table S1) including the coding exons and splice sites of 7 genes (*ATM, TP53, CCND1, WHSC1, KMT2D, NOTCH1* exon *34, BIRC3*) that are recurrently mutated in ≥ 5% of MCL tumors was specifically designed.[10-12] We also included in the

panel *TRAF2* [20] and *CXCR4.*[21] NGS libraries preparation was performed using TruSeq Custom Amplicon sequencing assay according to manufacturer's protocol (Illumina, Inc., San Diego, CA). Multiplexed libraries (n=48 per run) were sequenced using 300-bp paired-end runs on an Illumina MiSeq sequencer, (median depth of coverage 2356x). A robust and previously validated bioinformatics pipeline was used for variant calling (Supplementary Appendix). Copy number variation analysis methods[22,23] are supplied in the Supplementary Appendix.

Minimal residual disease analysis

For MRD purposes, MCL diagnostic BM and PB samples were investigated for IGH gene rearrangements and BCL1/IGH MTC by qualitative PCR.[24-26] Both BM and PB samples were analyzed for MRD at specific time points during and after treatment. Further information are supplied in the Supplementary appendix.

Statistical analysis

The primary outcome of the clinical study was progression-free survival (PFS) and secondary outcomes included overall survival (OS).[27] The adjusted effects of mutations and exposure variables (MIPI-c and blastoid variant) on PFS and OS were estimated by Cox regression. To compare clinical baseline features between patients enrolled in the molecular study and patients not included in the analysis, we used Mann-Whitney test for continuous variables and Pearson's chi-squared test for categorical variables. Statistical analyses were performed using Stata 13.0 and R 3.4.1. Further information are supplied in the Supplementary appendix.

Validation set

The Nordic Lymphoma Group “MCL2” and “MCL3”, phase 2, prospective trials[17] were used for independent validation of our findings. In particular, the raw sequencing data of the study by *Eskelund* were reanalyzed according to our bioinformatics pipeline (detailed before), to get a uniform mutation calling.

RESULTS

Patients characteristics

Out of the 300 patients enrolled in the FIL-MCL0208 clinical trial, 186 (62%) were provided with $CD19^+$ sorted tumor cells from the BM and evaluable for both mutations and copy number abnormalities. Moreover, four more patients were provided with the copy number abnormalities data only. Baseline features of cases included in the molecular study overlapped with those of cases not included in the molecular analysis because of lack of tumor material in the BM aspirates. As expected, tumor cells were obtained more frequently in cases with BM infiltration documented by morphological or flow-cytometry analysis (Table 1). Overall, this observation did not introduce a selection bias, since cases evaluable for genomic studies showed a similar outcome to that of cases not analyzed, both in terms of PFS and OS (Figure S1).

Description of genomic alterations

At least one somatic non-synonymous mutation affecting genes of the target region was observed in 69.8% of patients (130/186) (Figure 1, Figure S2; Table S2). Mutated genes were *ATM* (41.9%), followed by *WHSC1* (15.6%), *KMT2D* (12.4%), *CCND1* (11.8%), *TP53* (8.1%), *NOTCH1* (7.5%), *BIRC3* (5.9%) and *TRAF2* (1.1%). *KMT2D* deletion occurred in 1.6% of patients (3/190) and *TP53* deletion in 13.2% patients (25/190). *TP53* was inactivated by mutations or deletions in 31/186 (16.6%) cases, including 8/186 (4.3%) mutated/deleted cases, 16/186 (8.6%) deleted but not mutated cases, and 7/186 (3.7%) mutated but not deleted cases. *KMT2D* was inactivated by mutations or deletions in 25/186 (13.4%) cases, including 1/186 (<1%) mutated/deleted case, 2/186 (<1%) deleted but non mutated cases, and 22/186 (11.8%) mutated but not deleted cases.

***KMT2D* mutations and *TP53* disruption associate with poor outcome in MCL**

By univariate analysis, mutations of *KMT2D* were associated with poor clinical outcome in terms of both PFS and OS. At 4 years, the PFS of *KMT2D* mutated patients was 33.2% vs 63.7% ($p<0.001$) in wild type cases (Figure 2 A). The OS of *KMT2D* mutated patients was 62.3% vs 86.8% ($p=0.002$) in wild type patients (Figure 2 B). Consistent with previous reports, both *TP53* mutations and deletion associated with shorter PFS and OS at 4 years (Figure 2 C,D and Figure 3). In detail, the negative prognostic impact for *TP53* disruption was equal for all the three inactivation modalities, which were then considered as a single group for further analyses (Figure S3). No further survival analysis was performed on *KMT2D* deletions, given the low frequency of this genetic lesion. All the other investigated mutations did not show strong association with PFS or OS (Figures S4-6 and Table S3).

Patients harboring *TP53* disruption were significantly enriched in known high-risk features of MCL. Indeed, 48.3% of the *TP53* disrupted patients had Ki-67 ≥30%, 37.9% scored in the higher MIPI-c risk classes (i.e. “intermediate-high” and “high”), and 22.6% showed blastoid morphology. Conversely, 45.5% of cases harboring *KMT2D* mutations scored in the higher MIPI-c risk classes but did not associate with Ki-67 expression or blastoid morphology (Table S4). Moreover, *KMT2D* mutated patients showed slightly higher beta-2 microglobulin (B2M) median values, as well as higher prevalence of B symptoms and bulky disease (>5 cm) than wild type patients (all $p<0.05$). Interestingly, also *TP53* disrupted patients showed slightly higher B2M median values ($p<0.05$) than wild type patients (Table S4) and were associated with a high rate of disease progression during treatment (9 out of 31 patients, 29%). Moreover, *TP53* disrupted patients reached lower levels of MRD negativity after ASCT, if compared with wild type ones: 35% vs 58% in BM ($p=0.06$) and 58% vs 80% in PB ($p=0.04$), respectively. Similar trends were seen for *KMT2D* mutated patients (46% vs 55% in BM and 58% vs 79%), albeit not statistically significant (Table S5). Analogous to the Nordic

Lymphoma Group MCL2 and MCL3 trials[17], also in our study morphological BM involvement was significantly associated with the presence of mutations in any of the genes analysed ($p < 0.05$). However, both *TP53* disruptions and *KMT2D* mutations were equally distributed in patients with and without BM involvement ($p = 0.26$ and $p = 0.32$, respectively).

By multivariate analysis adjusted for the validated risk factors MIPI-c and blastoid variant, both *KMT2D* mutations and *TP53* disruptions maintained an independent increased hazard of progression and death (Table 2 and S6). Patients carrying at least one of these genetic lesions, namely *KMTD2* mutations, *TP53* mutations or deletion (n=49/186, 26.3%), had a 4-year PFS of 32.0% vs 69.9% of wild type patients ($p<0.0001$) and a 4-year OS of 65.1% vs 90.3% ($p<0.0001$), respectively (Figure 4).

Integration of a genetic score into the MIPI-c: the "MIPI-g" model

In order to integrate the clinical impact of *KMT2D* mutations and *TP53* disruptions into the MIPI-c prognostic index (complete data available for 172 patients), we assigned a score to each of the single variables, based on the multivariate Cox regression analysis. MIPI-c low, low-intermediate and intermediate-high risk classes scored 0 points, MIPI-c high-risk class scored 1 point, while *KMT2D* mutations as well as *TP53* disruption scored 2 points (Table 3). Patients were then grouped into three risk classes, according to their total score, in the "MIPI-genetic" index ("MIPI-g"), namely: *i)* 0 points, low risk group (LR 121 patients, 70.3%); *ii)* 1-2 points, intermediate risk group (IR 38 patients, 22.1%); *iii)* ≥3 points, high risk group (HR 13 patients, 7.6%). PFS and OS at 4-years for low-, intermediate-, and high-risk groups were 72.0%, 42.2%, 11.5% ($p<0.0001$) and 94.5%, 65.8%, 44.9% ($p<0.0001$), respectively (Figure 5). The MIPI-g index improved the model discrimination ability, with a C-statistics of 0.675 for PFS (bootstrapping corrected 0.654) and 0.776 for OS (bootstrapping corrected 0.747), as compared to MIPI-c alone (C-statistics 0.592 and 0.7, respectively).

Validation set

Most *KMT2D* variants considered in the Nordic study have been removed by our mutational calling, since these were missense variants not reported in COSMIC. At the end of the re-analysis, from the original 28 mutations, 21 were excluded. Two previously unrecognized frameshift mutations have been identified by our bioinformatics pipeline, overall accounting for a total of 9 *KMT2D* mutations (all disrupting, as expected for *KMT2D*) in the Nordic validation series. In the Nordic validation series, *KMT2D* mutated patients showed a similar increased risk for OS, with a median OS 12.7 years (95% C.I. not evaluable) for wild type vs. 8.4 (95% C.I 0-17.6) for mutated cases. The Nordic validation series also replicated the MIPI-g score. The re-analysis of *TP53* mutations confirmed the original data of Eskelund *et al*., with median OS of 12.7 (95% C.I. not evaluable) for wild type cases and 2.0 years (95% C.I, 1.2-2-8) for mutated cases. Consistently, also the MIPI-g validation on the Nordic series showed similar results: 4-year OS for LR (N=103), IR (N=36) and HR (N=13) MIPI-g groups were 91.3%, 72.2%, 15.4%.

DISCUSSION

To identify new molecular predictors in MCL, we performed targeted resequencing and DNA profiling of purified tumor samples collected from younger patients enrolled in the ASCT-based prospective FIL-MCL0208 phase III trial (NCT02354313). Our study documents that: *i) KMT2D* mutations are a novel, independent, adverse genetic biomarker in MCL, impacting both on PFS and OS (Figure 2 A,B); *ii) TP53* aberrations (both mutations and deletion) prospectively confirm their adverse prognostic value in younger MCL patients receiving high-dose chemo-immunotherapy followed by ASCT, both in terms of PFS and OS (Figures 2 C,D and Figure 3); *iii)* identification of either *KMT2D* mutations or *TP53* disruption (or both) defines a high-risk group of young MCL patients whose outcome is still not satisfactory despite intensive immunochemotherapy and ASCT (Figure 4); *iv)* these

biomarkers may be incorporated into a "genetic" MIPI-c ("MIPI-g") model, accounting for three risk classes (Figure 5), that improve the C-statistics discrimination ability on survival, if compared to MIPI-c alone.

The adverse prognostic value of *TP53* mutations in MCL has been already observed in some retrospective series,[13-17] and has been recently confirmed in a combined series from two, ASCT-based, phase II trials of the Nordic Lymphoma Group.[17] *TP53* deletions impacted on both PFS and OS in the randomized, phase III European MCL Network "Younger" trial,[16] while these data were not confirmed by multivariate analysis in the Nordic study, due to the high association with *TP53* mutations.[17] Our prospective study performed in a similar patient population of young MCL patients demonstrates that the presence of either *TP53* mutations or deletions or both associates with poor prognosis. Importantly, although *TP53* aberrations associated with elevated Ki-67, higher MIPI-c classes and blastoid morphology, their impact on survival was independent of these known risk factors. Moreover, *TP53* disrupted patients show higher levels of MRD positivity after ASCT, as described in Table S5. Finally, some previous studies reported also a negative impact of *NOTCH1* mutations in univariate analysis,[10,17] however in our cohort these mutations were not an independent predictor of survival, as most of them co-occurred with *TP53* mutations.

In the FIL-MCL0208 trial, *KMT2D* mutations emerged as a novel biomarker heralding chemo-immunotherapy failure, with a predictive value similar to that of *TP53* aberrations. *KMT2D* (Lysine Methyltransferase 2D), also known as *MLL2*, acts as a tumor suppressor gene mutated in several B-cell lymphoma types, including 10-15% of MCL.[28-31] Even though *KMT2D* mutated patients of the FIL-MCL0208 trial scored in the higher MIPI-c risk classes, they did not show either elevated Ki-67 or blastoid morphology, suggesting that *KMT2D* mutations capture high-risk patients not otherwise identifiable through conventional pathologic parameters.

To the best of our knowledge, the adverse impact on cancer survival of *KMT2D* mutations has not been documented to date. No impact on survival was found for *KMT2D* mutations in the Nordic study.[17] The lack of impact on survival of *KMT2D* mutations in the Nordic MCL series might be related to two main reasons. First, in the Nordic series, most *KMT2D* mutations were missense sequence variants (15/28) not reported as somatic variants in the COSMIC database, and therefore not fulfilling the criteria of "true" mutations. Conversely, in our series 74% of *KMT2D* mutations were protein truncating events, as expected[28-31]. Second, since Eskelund et al. performed mutational analysis in unsorted bone marrow samples, the low or absent tumor content of many cases might lead to underestimate *KMT2D* "true" mutations. By applying our bioinformatics pipeline to the raw sequencing data of the MCL2 and MCL3 Nordic Lymphoma Group trials, we validated the poor prognostic role of *KMT2D* mutations in an independent prospective cohort.

The independent adverse prognostic value of *TP53* and *KMT2D* aberrations prompted us to integrate the molecular results into the MIPI-c,[8] aiming at further improving its ability to discriminate high-risk patients. The "MIPI-genetic" ("MIPI-g") was able to divide patients into three risk classes, on the basis of a simple score given to each variable (namely: MIPI-c class, *TP53* disruption and *KMT2D* mutations). Patients in the high "MIPI-g" risk groups may deserve new treatments, and a simple tool like the MIPI-g might be proposed in a future, "tailored" trial to select high-risk MCL patients for targeted experimental strategies.

Our study suffers from some limitations. The analyses were performed only on CD19+ sorted BM cells and no tissue control is available at the moment; this issue might represent a limit for the extrapolation of the results to lymph-node samples, as across-compartment heterogeneity of the mutational landscape is described in MCL.[10] However, the CD19+ selection approach we used, increasing the purity of tumor cells and, consequently, the sensitivity of our mutational approach, ensured that all the analyzed samples are representative of MCL. Therefore, we set a VAF threshold of

10% to call a mutation, accordingly to ERIC guidelines for the mutational analysis of the *TP53* gene in chronic lymphocytic leukemia.[32] Although we acknowledge that the present validation relies on a limited number of *KMT2D* mutated patients, we note that the Nordic trials are currently the only prospective studies with prompt available mutational data, adequate clinical follow-up and similar characteristics (i.e. patients age and treatment schedule), to validate our original findings from the "FIL-MCL0208" trial.

The impact of lenalidomide maintenance in the FIL-MCL0208 trial on the described genetic aberrations has not been addressed, as complete data on randomization are not available yet. However, it should be noted that due to the high number of progressive diseases in the aberrant *TP53/KMT2D* group, 27 patients have been finally randomized but only 9 actually started lenalidomide maintenance. Therefore, it is unlikely that lenalidomide might play a clear role in driving the outcome of these patients and the trial will probably not be able to fully address this issue even with longer follow-up.

In conclusion, our results show that *KMT2D* mutated and/or *TP53* disrupted younger MCL patients are a high-risk population, characterized by poor sensitivity even to intensified chemo-immunotherapy. Given the negative prognostic impact of these genetic lesions, they might be used to select high-risk patients for novel therapeutic approaches that can circumvent these detrimental genetic lesions. As in other lymphoid disorders, novel non-chemotherapeutic strategies specifically designed for high-risk patients need to be investigated in MCL. Besides the approved drugs lenalidomide and ibrutinib, new molecules such as the Bcl-2 inhibitor venetoclax might be very promising for these chemorefractory patients, especially for *TP53* disrupted cases.[33,34] Moreover, as the majority of *KMT2D* mutated and/or *TP53* disrupted patients of our series actually achieve a response, though short-lasting after ASCT, an alternative consolidation with allogeneic transplantation deserves investigation.

REFERENCES

1. Eskelund CW, Kolstad A, Jerkeman M, et al. 15-year follow-up of the Second Nordic Mantle Cell Lymphoma trial (MCL2): prolonged remissions without survival plateau. Br J Haematol. 2016;175(3):410-418.
2. Hermine O, Hoster E, Walewski J, et al. Addition of high-dose cytarabine to immunochemotherapy before autologous stem-cell transplantation in patients aged 65 years or younger with mantle cell lymphoma (MCL Younger): a randomised, open-label, phase 3 trial of the European Mantle Cell Lymphoma Network. Lancet. 2016;388(10044):565-575.
3. Delarue R, Haioun C, Ribrag V, et al. CHOP and DHAP plus rituximab followed by autologous stem cell transplantation in mantle cell lymphoma: a phase 2 study from the Groupe d'Etude des Lymphomes de l'Adulte. Blood. 2013;121(1):48-53.
4. Romaguera JE, Fayad LE, Feng L, et al. Ten-year follow-up after intense chemoimmunotherapy with Rituximab-HyperCVAD alternating with Rituximab-high dose methotrexate/cytarabine (R-MA) and without stem cell transplantation in patients with untreated aggressive mantle cell lymphoma. Br J Haematol. 2010;150(2):200-208.
5. Le Gouill S, Thieblemont C, Oberic L, et al. Rituximab after Autologous Stem-Cell Transplantation in Mantle-Cell Lymphoma. N Engl J Med. 2017;377(13):1250-1260.
6. Hoster E, Dreyling M, Klapper W, et al. A new prognostic index (MIPI) for patients with advanced-stage mantle cell lymphoma. Blood. 2008;111(2):558-565.
7. Hoster E, Klapper W, Hermine O, et al. Confirmation of the mantle-cell lymphoma International Prognostic Index in randomized trials of the European Mantle-Cell Lymphoma Network. J Clin Oncol. 2014;32(13):1338-1346.

8. Hoster E, Rosenwald A, Berger F, et al. Prognostic value of Ki-67 index, cytology, and growth pattern in mantle-cell lymphoma: Results from randomized trials of the european mantle cell lymphoma network. J Clin Oncol. 2016;34(12):1386-1394.
9. Dreyling M, Ferrero SE. The role of targeted treatment in mantle cell lymphoma: Is transplant dead or alive? Haematologica. 2016;101(2):104-114.
10. Beà S, Valdés-Mas R, Navarro A, et al. Landscape of somatic mutations and clonal evolution in mantle cell lymphoma. Proc Natl Acad Sci U S A. 2013;110(45):18250-18255.
11. Zhang J, Jima D, Moffitt AB, et al. The genomic landscape of mantle cell lymphoma is related to the epigenetically determined chromatin state of normal B cells. Blood. 2014;123(19):2988-2996.
12. Rahal R, Frick M, Romero R, et al. Pharmacological and genomic profiling identifies NF-κB-targeted treatment strategies for mantle cell lymphoma. Nat Med. 2014;20(1):87-92.
13. Kumar A, Yang W, Bantilan KS, et al. Prognostic Significance of Genomic Alterations in Mantle Cell Lymphoma. Blood. 2016;128(22):4115.
14. Nordström L, Sernbo S, Eden P, et al. SOX11 and TP53 add prognostic information to MIPI in a homogenously treated cohort of mantle cell lymphoma - a Nordic Lymphoma Group study. Br J Haematol. 2014;166(1):98-108.
15. Halldórsdóttir AM, Lundin A, Murray F, et al. Impact of TP53 mutation and 17p deletion in mantle cell lymphoma. Leukemia. 2011;25(12):1904-1908.
16. Delfau-Larue MH, Klapper W, Berger F, et al. High-dose cytarabine does not overcome the adverse prognostic value of CDKN2A and TP53 deletions in mantle cell lymphoma. Blood. 2015;126(5):604-611.

17. Eskelund CW, Dahl C, Hansen JW, et al. TP53 mutations identify younger mantle cell lymphoma patients who do not benefit from intensive chemoimmunotherapy. Blood. 2017;130(17):1903-1910.
18. Cortelazzo S, Martelli M, Ladetto M, et al. High Dose Sequential Chemotherapy with Rituximab and ASCT as First Line Therapy in Adult MCL Patients: Clinical and Molecular Response of the MCL0208 Trial, a FIL Study. Haematologica. 2015;100(s1):3-4.
19. Swerdlow SH, Campo E, Pileri SA, et al. The 2016 revision of the World Health Organization classification of lymphoid neoplasms. Blood. 2016;127(20):2375-2390
20. Meissner B, Kridel R, Lim RS, et al. The E3 ubiquitin ligase UBR5 is recurrently mutated in mantle cell lymphoma. Blood. 2013;121(16):3161-3164.
21. Roccaro AM, Sacco A, Jimenez C, et al. C1013G/CXCR4 acts as a driver mutation of tumor progression and modulator of drug resistance in lymphoplasmacytic lymphoma. Blood. 2014;123(26):4120-4131.
22. Rinaldi A, Kwee I, Young KH, et al. Genome-wide high resolution DNA profiling of hairy cell leukaemia. Br J Haematol. 2013;162(4):566-569.
23. Kwee IW, Rinaldi A, de Campos CP, et al. Fast and Robust Segmentation of Copy Number Profiles Using Multi-Scale Edge Detection. BioRxiv. 2016. https://doi.org/10.1101/056705.
24. Voena C, Ladetto M, Astolfi M, et al. A novel nested-PCR strategy for the detection of rearranged immunoglobulin heavy-chain genes in B cell tumors. Leukemia. 1997;11(10):1793-1798.
25. Stamatopoulos K, Kosmas C, Belessi C, et al. Molecular analysis of bcl-1/IgH junctional sequences in mantle cell lymphoma: potential mechanism of the t(11;14) chromosomal translocation. Br J Haematol. 1999;105(1):190-197.

26. Pott C. Minimal residual disease detection in mantle cell lymphoma: technical aspects and clinical relevance. Semin Hematol. 2011;48(3):172-184.
27. Cheson BD, Pfistner B, Juweid ME, et al. Revised response criteria for malignant lymphoma. J Clin Oncol. 2007;25(5):579-586.
28. Froimchuk E, Jang Y, Ge K. Histone H3 lysine 4 methyltransferase KMT2D. Gene. 2017;627:337-342.
29. Varettoni M, Zibellini S, Defrancesco I, et al. Pattern of somatic mutations in patients with Waldenström macroglobulinemia or IgM monoclonal gammopathy of undetermined significance. Haematologica. 2017;102(12):2077-2085.
30. Spina V, Khiabanian H, Messina M, et al. The genetics of nodal marginal zone lymphoma. Blood. 2016;128(10):1362-1373.
31. Pasqualucci L, Trifonov V, Fabbri G, et al. Analysis of the coding genome of diffuse large B-cell lymphoma. Nat Genet. 2011;43(9):830-837.
32. Malcikova J, Tausch E, Rossi D, et al. ERIC recommendations for TP53 mutation analysis in chronic lymphocytic leukemia-update on methodological approaches and results interpretation. Leukemia. 2018;32(5):1070-1080.
33. Davids MS, Roberts AW, Seymour JF, et al. Phase I First-in-Human Study of Venetoclax in Patients With Relapsed or Refractory Non-Hodgkin Lymphoma. J Clin Oncol. 2017;35(8):826-833.
34. Tam CS, Anderson MA, Pott C, et al. Ibrutinib plus Venetoclax for the Treatment of Mantle-Cell Lymphoma. N Engl J Med. 2018;378(13):1211-1223.

Table 1. Clinical and biological baseline characteristics of the patients included and not included in the molecular analysis

Characteristics	Patients analysed for mutations and/or CNV (N=190)	Patients not analysed for mutations and CNV (N=110)	*P*-value
Median age	57	58	0.987
Gender			
Female	47 (24.7%)	18 (16.4%)	0.090
Male	143 (75.3%)	92 (83.6%)	
Ki-67			
<30%	126 (71.6%)	61 (64.2%)	0.210
≥30%	50 (28.4%)	34 (35.8%)	
Median WBC	74500/ul	75000/ul	0.567
ECOG			
0	144 (75.8%)	87 (79.2%)	0.722
1	40 (21.1%)	19 (17.3%)	
2	6 (3.2%)	4 (3.6%)	
Median LDH	275.5 UI/L	298	0.848
Risk class MIPI			
Low	114 (60.0%)	66 (60.0%)	0.562
Intermediate	49 (25.8%)	24 (21.8%)	
High	27 (14.2%)	20 (18.2%)	
Risk class MIPI-c			
Low	88 (50.0%)	45 (47.4%)	0.685
Low-Intermediate	49 (27.8%)	30 (31.6%)	
Intermediate/High	25 (14.2%)	10 (10.5%)	
High	14 (8.0%)	10 (10.5%)	
BM Invasion			
No	26 (13.9%)	37 (33.9%)	<0.001
Yes	161 (86.1%)	72 (66.1%)	
Median BM invasion by flow (%)	10%	0.8%	<0.0001
Histology			
MCL Classic	174 (91.6%)	100 (90.9%)	0.842
MCL blastoid variant	16 (8.4%)	10 (9.1%)	
Bulky mass			
No	124 (65.3%)	78 (70.9%)	0.315
Yes	66 (34.7%)	32 (29.1%)	

CNV, Copy Numer Variation Analysis; WBC, White Blood Cells; ECOG, Eastern Cooperative Oncology Group; LDH, Lactate dehydrogenase; MIPI, MCL International Prognostic Index; MIPI-c, Combined MIPI; BM, Bone Marrow

Table 2. Uniavariate and multivariate Cox-regression analysis in terms of PFS an OS

	Progression free survival						Overall survival					
	Univariate			Multivariate (MIPI-c and blastoid variant adjusted)			Univariate			Multivariate (MIPI-c and blastoid variant adjusted)		
Genes	HR	*95% CI*	*P*-value	HR	*95% CI*	*P*-value	HR	*95% CI*	*P*-value	HR	*95% CI*	*P*-value
ATM mut	1.29	0.84-1.97	0.245	1.19	0.77-1.83	0.432	1.52	0.62-2.51	0.527	1.05	0.52-2.12	0.887
WHSC1 mut	1.53	0.90-2.60	0.119	1.51	0.87-2.61	0.140	0.85	0.30-2.41	0.755	0.741	0.25-2.15	0.581
CCND1 mut	0.83	0.41-1.66	0.595	0.94	0.46-1.92	0.860	0.75	0.23-2.48	0.643	1.01	0.29-3.53	0.980
KMT2D mut	2.59	1.50-4.48	0.001	2.74	1.55-4.84	0.001	3.20	1.48-6.92	0.003	2.48	1.12-5.46	0.024
TP53 mut	2.84	1.57-5.13	0.001	2.55	1.36-4.78	0.003	5.28	2.44-11.45	<0.0001	2.78	1.09-7.06	0.032
NOTCH1 mut	1.86	0.93-3.72	0.078	1.57	0.76-3.24	0.226	1.34	0.41-4.40	0.629	0.61	0.17-2.12	0.609
BIRC3 mut	0.88	0.32-2.41	0.807	0.70	0.25-1.96	0.500	1.84	0.56-6.08	0.315	1.15	0.33-3.98	0.822
TP53 del	3.51	2.09-5.88	<0.0001	3.13	1.73-5.68	<0.001	4.46	2.14-9.29	<0.0001	2.65	1.06-6.59	0.036
TP53 dis	3.39	2.10-5.45	<0.0001	3.17	1.87-5.38	<0.0001	4.26	2.09-8.67	<0.0001	2.65	1.10-6.37	0.030

Del, deleted; dis, disrupted; PFS, Progression Free Survival; OS, overall survival; HR, Hazard Ratio; CI, Confidence Interval.

Table 3. The MIPI-g score

Variables	Beta-coefficients	Points
***KMT2D* mutations**	1,035,607	2
***TP53* disruption**	1,113,875	2
MIPI-c		
Low	-	0
Low-Intermediate	-	0
Intermediate-High	-	0
High	0.6847757	1

MIPI-c, Combined Mantle Cell International Prognostic Index

FIGURE LEGENDS

Figure 1. Overview on prevalence and molecular spectrum of non-synonymous somatic mutations discovered in patients' tumor DNA. Heatmap representing the mutational profiles of 186 MCL cases, genotyped on tumor DNA (and four additional patients with copy number abnormalities data only). Each column represents one patient, each row represents one gene. The fraction of patients with mutations in each gene is plotted on the right. The number of aberrations in a given patient is plotted above the heatmap.

Figure 2. Prognostic impact of *KMT2D* and *TP53* mutations. Kaplan-Meier estimates of progression free survival and overall survival of *KMT2D* (A, B), and *TP53* (C, D) mutated versus wild type patients. Cases harboring mutations (mut) in these genes are represented by the yellow line. Cases wild type (wt) for these genes are represented by the blue line. The Log-rank statistics *p* values are indicated adjacent curves.

Figure 3. Prognostic impact of *TP53* deletion. Kaplan-Meier estimates of progression free survival (A) and overall survival (B) of *TP53* deleted versus wild type patients. Cases with *TP53* deletion are represented by the yellow line. Cases without *TP53* deletion are represented by the blue line. The Log-rank statistics *p* values are indicated adjacent curves.

Figure 4. Prognostic impact of combined *KMT2D* mutations and *TP53* disruption. Kaplan-Meier estimates of (A) progression free survival and (B) overall survival of patients harboring *KMT2D* mutations and/or *TP53* disruption (mutations and/or deletions). Cases harboring at least one of these 3 genetic lesions are represented by the yellow line. Cases without these genes are represented by the blue line. The Log-rank statistics *p* values are indicated adjacent curves.

Figure 5. The "MIPI-g" model. Kaplan-Meier estimates of (A) progression free survival and (B) overall survival of patients harboring *KMT2D* mutations and/or *TP53* disruption (mutations and/or deletions) integrated into the MIPI-c. Low MIPI-g risk cases are represented by the blue line, intermediate MIPI-g cases by the yellow line and high MIPI-g cases by the red line. The Log-rank statistics *p* values are indicated adjacent curves.

Figure 1

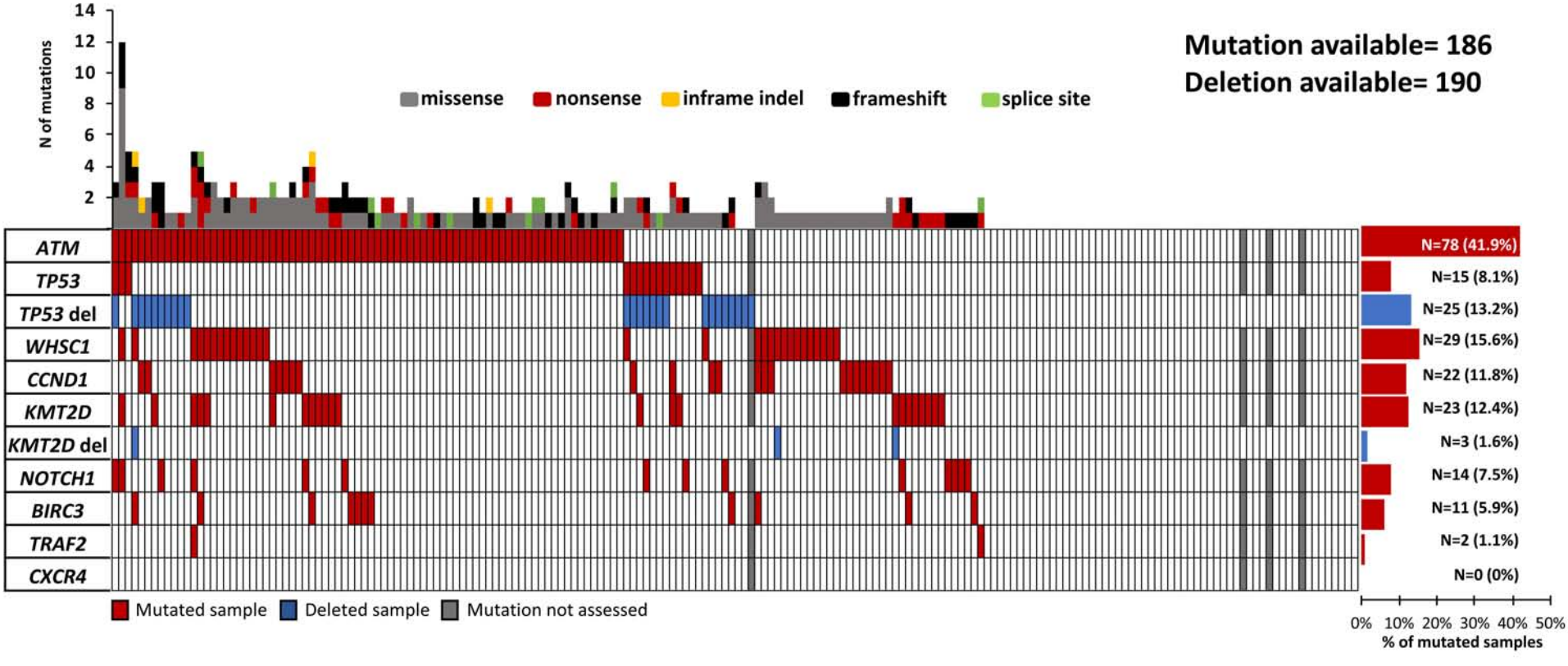
N of mutations
14
12
10
8
6
4
2
missense
nonsense
inframe indel
frameshift
splice site
Mutation available= 186
Deletion available= 190
ATM
TP53
TP53 del
WHSC1
CCND1
KMT2D
KMT2D del
NOTCH1
BIRC3
TRAF2
CXCR4
N=78 (41.9%)
N=15 (8.1%)
N=25 (13.2%)
N=29 (15.6%)
N=22 (11.8%)
N=23 (12.4%)
N=3 (1.6%)
N=14 (7.5%)
N=11 (5.9%)
N=2 (1.1%)
N=0 (0%)
Mutated sample
Deleted sample
Mutation not assessed
0% 10% 20% 30% 40% 50%
% of mutated samples

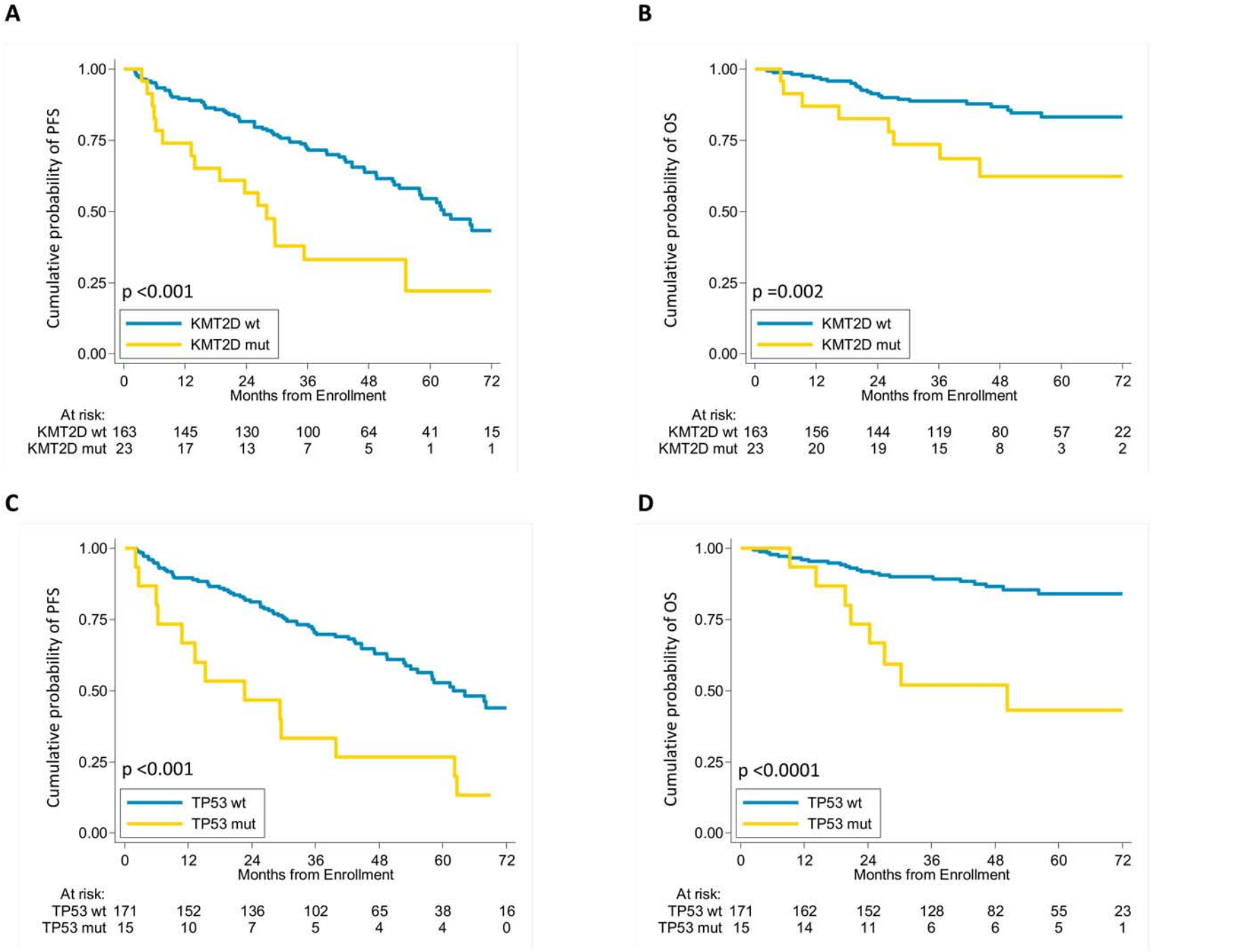
A
Cumulative probability of PFS
1.00
0.75
0.50
0.25
0.00
p <0.001
KMT2D wt
KMT2D mut
0 12 24 36 48 60 72
Months from Enrollment
At risk:
KMT2D wt 163 145 130 100 64 41 15
KMT2D mut 23 17 13 7 5 1 1
B
Cumulative probability of OS
1.00
0.75
0.50
0.25
0.00
p =0.002
KMT2D wt
KMT2D mut
0 12 24 36 48 60 72
Months from Enrollment
At risk:
KMT2D wt 163 156 144 119 80 57 22
KMT2D mut 23 20 19 15 8 3 2
C
Cumulative probability of PFS
1.00
0.75
0.50
0.25
0.00
p <0.001
TP53 wt
TP53 mut
0 12 24 36 48 60 72
Months from Enrollment
At risk:
TP53 wt 171 152 136 102 65 38 16
TP53 mut 15 10 7 5 4 4 0
D
Cumulative probability of OS
1.00
0.75
0.50
0.25
0.00
p <0.0001
TP53 wt
TP53 mut
0 12 24 36 48 60 72
Months from Enrollment
At risk:
TP53 wt 171 162 152 128 82 55 23
TP53 mut 15 14 11 6 6 5 1

Figure 2

Figure 3

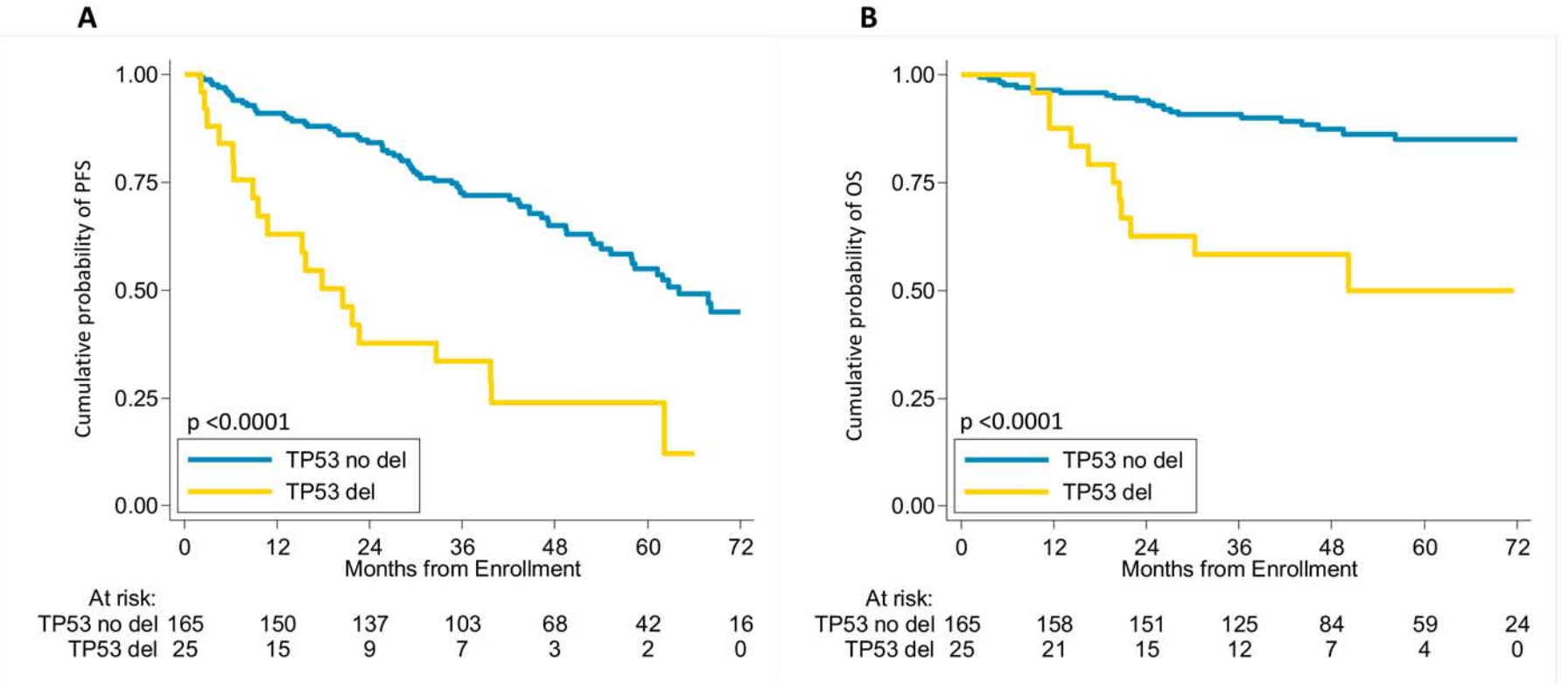
A
1.00
0.75
0.50
0.25
0.00
Cumulative probability of PFS
p <0.0001
TP53 no del
TP53 del
0
12
24
36
48
60
72
Months from Enrollment
At risk:
TP53 no del 165 150 137 103 68 42 16
TP53 del 25 15 9 7 3 2 0
B
1.00
0.75
0.50
0.25
0.00
Cumulative probability of OS
p <0.0001
TP53 no del
TP53 del
0
12
24
36
48
60
72
Months from Enrollment
At risk:
TP53 no del 165 158 151 125 84 59 24
TP53 del 25 21 15 12 7 4 0

Figure 4

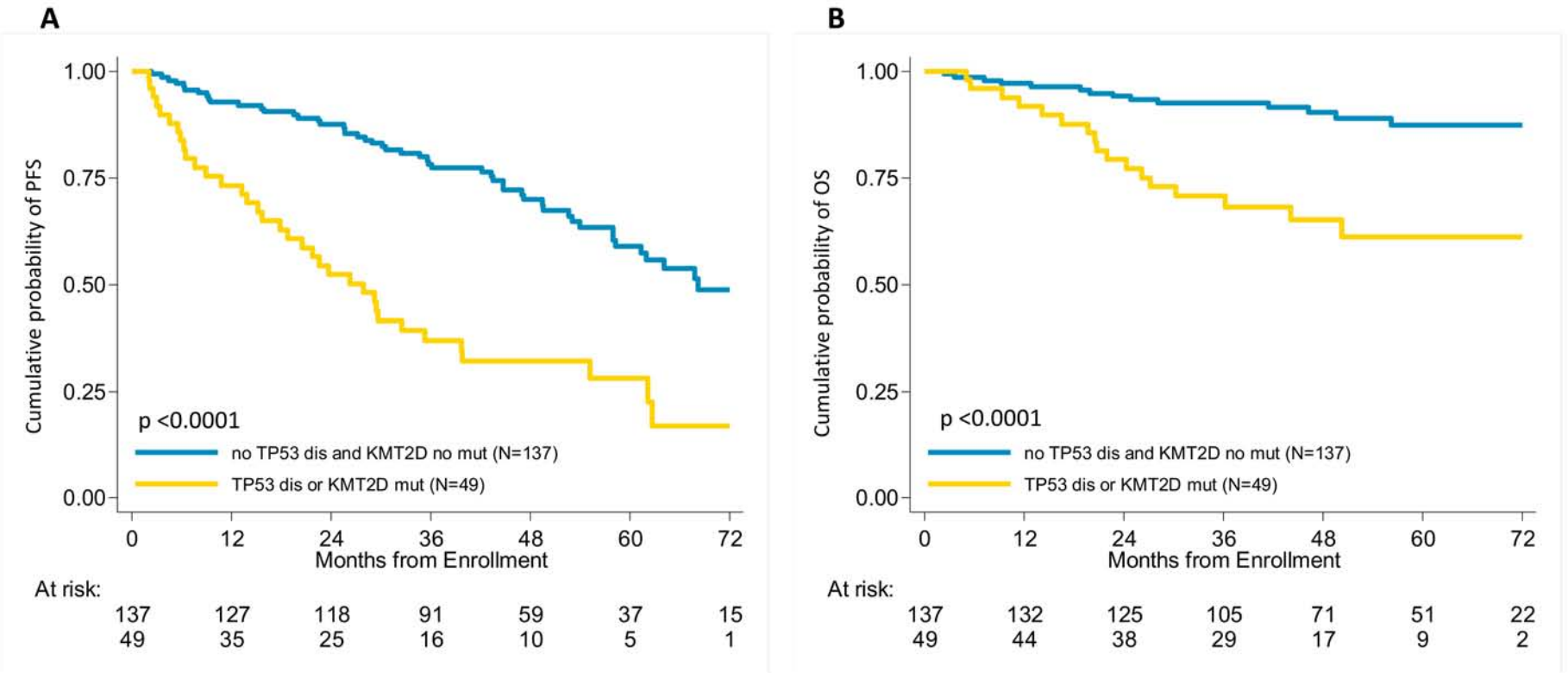
A
1.00
0.75
0.50
0.25
0.00
Cumulative probability of PFS
p <0.0001
no TP53 dis and KMT2D no mut (N=137)
TP53 dis or KMT2D mut (N=49)
0
12
24
36
48
60
72
Months from Enrollment
At risk:
137 127 118 91 59 37 15
49 35 25 16 10 5 1
B
1.00
0.75
0.50
0.25
0.00
Cumulative probability of OS
p <0.0001
no TP53 dis and KMT2D no mut (N=137)
TP53 dis or KMT2D mut (N=49)
0
12
24
36
48
60
72
Months from Enrollment
At risk:
137 132 125 105 71 51 22
49 44 38 29 17 9 2

Figure 5

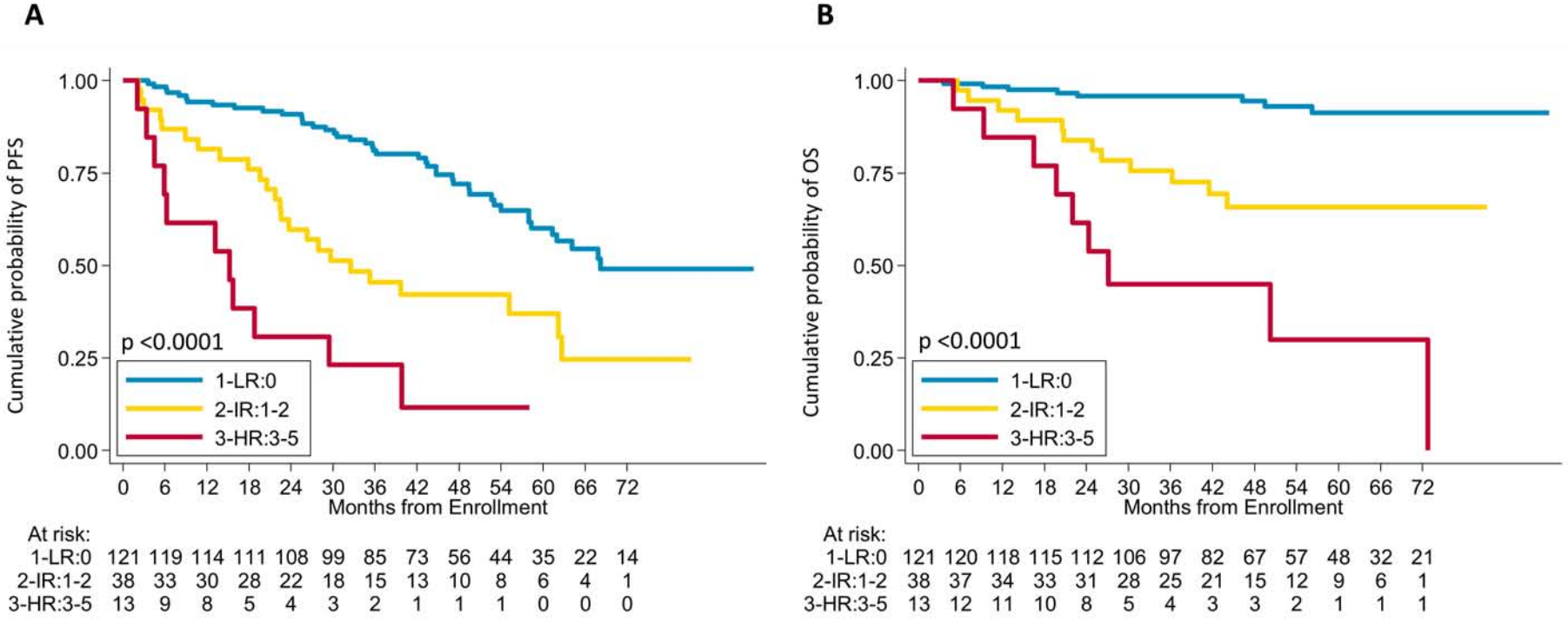
A
Cumulative probability of PFS
1.00
0.75
0.50
0.25
0.00
p <0.0001
1-LR:0
2-IR:1-2
3-HR:3-5
0 6 12 18 24 30 36 42 48 54 60 66 72
Months from Enrollment
At risk:
1-LR:0 121 119 114 111 108 99 85 73 56 44 35 22 14
2-IR:1-2 38 33 30 28 22 18 15 13 10 8 6 4 1
3-HR:3-5 13 9 8 5 4 3 2 1 1 1 0 0 0
B
Cumulative probability of OS
1.00
0.75
0.50
0.25
0.00
p <0.0001
1-LR:0
2-IR:1-2
3-HR:3-5
0 6 12 18 24 30 36 42 48 54 60 66 72
Months from Enrollment
At risk:
1-LR:0 121 120 118 115 112 106 97 82 67 57 48 32 21
2-IR:1-2 38 37 34 33 31 28 25 21 15 12 9 6 1
3-HR:3-5 13 12 11 10 8 5 4 3 3 2 1 1 1

SUPPLEMENTARY APPENDIX

KMT2D mutations and *TP53* disruptions are poor prognostic biomarkers in MCL receiving high-dose therapy: a FIL study

Simone Ferrero[*1,2], Davide Rossi*[*3,4], Andrea Rinaldi*[*4], Alessio Bruscaggin[4], Valeria Spina[4], Christian W Eskelund[5,6], Andrea Evangelista[7], Riccardo Moia[8], Ivo Kwee[4,9,10], Christina Dahl[11], Alice Di Rocco[12], Vittorio Stefoni[13], Fary Diop[8], Chiara Favini[8], Paola Ghione[1], Abdurraouf Mokhtar Mahmoud[8], Mattia Schipani[8], Arne Kolstad[14], Daniela Barbero[1], Domenico Novero[15], Marco Paulli[16], Alberto Zamò[17,18], Mats Jerkeman[19], Maria Gomes da Silva[20], Armando Santoro[21], Annalia Molinari[22], Andres Ferreri[23], Kirsten Grønbæk[5,6], Andrea Piccin[24], Sergio Cortelazzo[25], Francesco Bertoni°[4], Marco Ladetto°[26] and Gianluca Gaidano°[8]*

[1]Department of Molecular Biotechnologies and Health Sciences - Hematology Division, Università di Torino, Torino, Italy; [2]Hematology Division, AOU Città della Salute e della Scienza di Torino, Torino, Italy; [3]Hematology, Oncology Institute of Southern Switzerland, Bellinzona, Switzerland; [4]Universita' della Svizzera italiana, Institute of Oncology Research, Bellinzona, Switzerland; [5]Department of Hematology, Rigshospitalet, Copenhagen, Denmark; [6]Biotech Research and Innovation Centre, Copenhagen, Denmark; [7]Clinical Epidemiology, Città della Salute e della Scienza and CPO Piemonte, Torino, Italy; [8]Division of Hematology, Department of Translational Medicine, University of Eastern Piedmont, Novara, Italy; [9]Swiss Institute of Bioinformatics (SIB), Lausanne, Switzerland; [10]Dalle Molle Institute for Artificial Intelligence (IDSIA), Manno, Switzerland; [11]Danish Cancer Society Research Center, Copenhagen, Denmark; [12]Department of Cellular Biotechnologies and Hematology, Policlinico Umberto I, "Sapienza" University of Rome, Roma, Italy; [13]Institute of Hematology "L. e A. Seràgnoli", University of Bologna, Bologna, Italy; [14]Department of Oncology, Oslo University Hospital, Oslo, Norway; [15]First unit of Pathology, AOU

Città della Salute e della Scienza di Torino, Torino, Italy; [16]Unit of Anatomic Pathology, Department of Molecular Medicine, Fondazione IRCCS Policlinico San Matteo and Università degli Studi di Pavia, Pavia, Italy; [17]Department of Oncology, Università di Torino, Torino, Italy; [18]Department of Diagnostics and Public Health, University of Verona, Italy; [19]Department of Oncology, Lund University Hospital, Lund, Sweden; [20]Department of Hematology, Instituto Português de Oncologia de Lisboa, Lisboa, Portugal; [21]Humanitas Cancer Center, Humanitas Clinical and Research Center, Rozzano, Italy; [22]Hematology, Ospedale degli Infermi, Rimini, Italy; [23]Lymphoma Unit, Department of Onco-Haematology, IRCCS San Raffaele Scientific Institute, Milano, Italy; [24]Department of Hematology, Ospedale Generale, Bolzano, Italy; [25]Oncology Unit, Humanitas/Gavazzeni Clinic, Bergamo, Italy; [26]SC Ematologia, Azienda Ospedaliera Santi Antonio e Biagio e Cesare Arrigo, Alessandria, Italy.

* These Authors equally contributed as First Authors

° These Authors equally contributed as Senior Authors

SUPPLEMENTARY METHODS

Patients series

The FIL-MCL0208 (NCT02354313) is a phase III, multicenter, open-label, randomized, controlled study, designed to determine the efficacy of lenalidomide as maintenance versus observation in young (18-65 years old), fit, advanced stage (Ann arbor II-IV) MCL patients who achieved complete or partial remission after first line intensified and high-dose chemotherapy plus rituximab followed by ASCT. Briefly, patients received 3 R-CHOP-21, followed by R-high-dose cyclophosphamide (4g/m2), 2 cycles of R-high-dose Ara-C (2g/m2 q12x3 d) and ASCT conditioned by using the BEAM or FEAM regimen. From May 2010 to August 2015, a total of 300 patients were enrolled in the study. Cases of non-nodal MCL were excluded.[1] All patients required to have a biopsy proving MCL, including evidence of cyclin D1 overexpression or t(11;14)(q13;q32) translocation. MCL diagnosis was confirmed by centralized pathological revision according to WHO criteria.[1] The clinical trial, as well as the ancillary mutational study, were approved by the Ethical Committees of all the enrolling Centers. All patients provided written informed consent for the use of their biological samples for research purposes, in accordance with Institutional Review Boards requirements and the Helsinki's declaration. Clinical results of the fist interim analysis of the trial were already presented.[2] Final, unblinded results are not available at the moment and have not been yet presented anywhere.

Biological samples

Bone marrow (BM) and peripheral blood (PB) samples were collected, as per protocol, at baseline and at several time-points during follow-up, corresponding to the pre-planned time-points for minimal residual disease (MRD) analysis. To identify and quantify the rate of tumor invasion, flow cytometry (FC) was performed both on BM and PB with the following antibodies: anti-CD19 APC, anti-CD23 PE, anti-CD5 FITC, and anti-CD20. Tumor cells were sorted from the baseline BM

samples by immunomagnetic beads (CD19 MicroBeads,human-Miltenyi Biotec GmbH, Bergisch Gladbach, Germany) and stocked as dry pellets.

Tumor DNA was extracted according to DNAzol protocol (Life Technologies). Germline DNA was obtained from PB mononuclear cells collected under treatment and proven to be tumor free by MRD analysis.

Next generation sequencing

A targeted resequencing panel (target region: 37'821 bp) (Table S1) including the coding exons and splice sites of 7 genes (*ATM, TP53, CCND1, WHSC1, KMT2D, NOTCH1* exon *34, BIRC3*) that are recurrently mutated in ≥ 5% of MCL tumors was specifically designed.[3-5] We also included in the panel *TRAF2* [6] and *CXCR4.*[7] The gene panel was analyzed in tumor DNA from baseline BM $CD19^+$ purified MCL cells (186 cases) and, for comparative purposes to filter out polymorphisms, in the paired normal genomic DNA (105 cases). NGS libraries preparation was performed using TruSeq Custom Amplicon sequencing assay according to manufacturer's protocol (Illumina, Inc., San Diego, CA). Multiplexed libraries (n=48 per run) were sequenced using 300-bp paired-end runs on an Illumina MiSeq sequencer, (median depth of coverage 2356x). To avoid the loss of *NOTCH1* ex 34 c.7544_7545delCT mutation, that is included in a region poorly covered by the target design, all MCL cases were also analyzed by amplification refractory mutation system (ARMS) polymerase chain reaction (PCR).

Bioinformatic analysis

FASTQ sequencing reads were locally aligned to the hg19 version of the human genome assembly using the BWA v.0.6.2 software with the default setting, and sorted, indexed and assembled into a mpileup file using SAMtools v.1. The aligned read families were processed with mpileup. A cut-off of 10% of variant allele frequency (VAF) was set for variant calling. Among cases provided with both tumor and paired normal gDNA, single nucleotide variations and indels were called using

the somatic function of VarScan2. The variants called by VarScan2 were annotated by using the SeattleSeq Annotation 138 tool by using the default setting. Variants annotated as SNPs according to dbSNP 138 (with the exception of *TP53* variants that were manually curated and scored as SNPs according to the IARC *TP53* database), intronic variants mapping >2 bp before the start or after the end of coding exons, and synonymous variants were then filtered out. The following strict post-processing filters were then applied to the remaining variants to further improve variant call confidence. Accordingly, variants represented in >10 reads of the paired germline and/or variants with a somatic p value from VarScan2 >$3.305e^{-7}$ [multiple comparisons corrected p threshold=$3.305e^{-7}$, corresponding to alpha of 0.05/(37'821 x 4 alleles per position)] were no further considered. Variant allele frequencies for the resulting candidate mutations and the background error rate were visualized using IGV. Among patients lacking the paired normal gDNA, single nucleotide variations and indels were called in tumor gDNA with the *cns* function of VarScan2. The variants called by VarScan2 were annotated by using the SeattleSeq Annotation 138 tool by using the default setting. Variants annotated as SNPs according to dbSNP 138 (with the exception of *TP53* variants that were manually curated and scored as SNPs according to the IARC *TP53* database), intronic variants mapping >2 bp before the start or after the end of coding exons, and synonymous variants were then filtered out. Only protein truncating variants (i.e. indels, stop codons and splice site mutations), as well as missense variants not included in the dbSNP 138 and annotated as somatic in the COSMIC v78 database, were retained.

Copy number variation analysis

DNA profiling was performed on DNA samples derived from baseline BM CD19+ purified tumor cells using the HumanOmni2.5 arrays (Illumina, San Diego, CA, USA). Copy number status of the genes included in the targeted resequencing panel (*KMT2D* and *TP53*) was assessed after genomic profiles segmentation with the Fast First-derivative Segmentation Algorithm, as previously described.[8,9]

Minimal residual disease analysis

For MRD purposes, MCL diagnostic BM and PB samples were investigated for IGH gene rearrangements and BCL1/IGH MTC by qualitative PCR. Briefly, IGH were screened using forward consensus primers annealing the IGH-V-regions and a reverse primer complementary to the JH region. BCL1/IGH MTC translocation was investigated by nested-PCR approach, as described.[10-12] After direct sequencing, FASTA files alignment was performed by IMGT/V-QUEST (http://imgt.org) and BlastN tool (NCBI, https://blast.ncbi.nlm.nih.gov/Blast.cgi), in order to define rearranged loci nomenclature, chromosomic breakpoints, and to assess patient specific nucleotide insertions (N insertions), then used to design allele specific oligonucleotides primers for nested-PCR MRD monitoring. Therefore, both BM and PB samples were analyzed for MRD at specific time points during and after treatment.

Statistical analysis

The primary outcome of the clinical study was progression-free survival (PFS). PFS was calculated from the date of enrolment into the clinical study to the date of disease progression (event), death from any causes (event), or last follow up (censoring).[13] Secondary outcomes included overall survival (OS), measured from the date of enrolment into the clinical study to the date of death from any causes (event), or last follow up (censoring). Time-to-event outcomes (PFS and OS) were estimated using the Kaplan-Meier method and compared between groups using the Log-rank test. The adjusted effects of mutations and exposure variables (MIPI-c and blastoid variant) on PFS and OS were estimated by Cox regression. To compare clinical baseline features between patients enrolled in the molecular study and patients not included in the analysis, we used Mann-Whitney test for continuous variables and Pearson's chi-squared test for categorical variables. A Cox model for PFS was estimated including MIPI-c and clinically impacting genetic alterations, and an additive score was computed according to the proportion between each predictor coefficient and the lowest one. The Cox model was internally validated using 1000 bootstrap samples and the C-statistic correct

for optimism was also provided. Patients were then grouped in classes of risk according to their total score using the nonparametric tree modelling technique of classification and regression tree (CART) analysis. Statistical analyses were performed using Stata 13.0 and R 3.4.1. The outcome data for the present analysis were updated as of December, 2017 the randomization arms being still blinded.

SUPPLEMENTARY FIGURE LEGENDS

Figure S1. Survival analysis for patients enrolled in the MCL0208 clinical trial included and not included in the present molecular study. Kaplan-Meier estimates of progression free survival (A) and overall survival (B) of patients with available DNA included in the present molecular study (in blue) and of patients without available DNA not included in the present molecular study (in yellow). The Log-rank statistics *p* values are indicated adjacent curves.

Figure S2. Disposition of identified gene mutations across the protein. Mutations identified in the studied cohort are plotted above the protein divided into the main domains**.** Missense mutations are plotted in green, stop codon mutations in red, splicing mutations in black, frameshift mutations in red, in-frame mutations in yellow.

Figure S3. Prognostic impact of *TP53* mutation and *TP53* deletion. Kaplan-Meier estimates of progression free survival (A) and overall survival (B) of *TP53* mutated patients, *TP53* deleted patients, *TP53* mutated and deleted patients, versus wild type patients. Cases with *TP53* mutation are represented by the yellow line, cases with *TP53* deletion are represented by the red line, cases with *TP53* mutation and deletion are represented by the black line, cases without *TP53* mutation and deletion are represented by the blue line. The Log-rank statistics *p* values are indicated adjacent curves.

Figure S4. Prognostic impact of *NOTCH1* mutation and *ATM* mutation. Kaplan-Meier estimates of (A) progression free survival and (B) overall survival of patients harboring *NOTCH1* mutation and Kaplan-Meier estimates of (C) progression free survival and (D) overall survival of patients harboring *ATM* mutation. Cases harboring *NOTCH1* or *ATM* mutation are represented by the yellow line. Wild

type cases are represented by the blue line. The Log-rank statistics *p* values are indicated adjacent curves.

Figure S5. Prognostic impact of *WHSC1* mutation and *CCND1* mutation. Kaplan-Meier estimates of (A) progression free survival and (B) overall survival of patients harboring *WHSC1* mutations and Kaplan-Meier estimates of (C) progression free survival and (D) overall survival of patients harboring *CCND1* mutation. Cases harboring *WHSC1* or *CCND1* mutation are represented by the yellow line. Wild type cases are represented by the blue line. The Log-rank statistics *p* values are indicated adjacent curves.

Figure S6. Prognostic impact of *BIRC3* mutation and *TRAF2* mutation. Kaplan-Meier estimates of (A) progression free survival and (B) overall survival of patients harboring *BIRC3* mutation and Kaplan-Meier estimates of (C) progression free survival and (D) overall survival of patients harboring *TRAF2* mutation. Cases harboring *BIRC3* or *TRAF2* mutation are represented by the yellow line. Wild type cases are represented by the blue line. The Log-rank statistics *p* values are indicated adjacent curves.

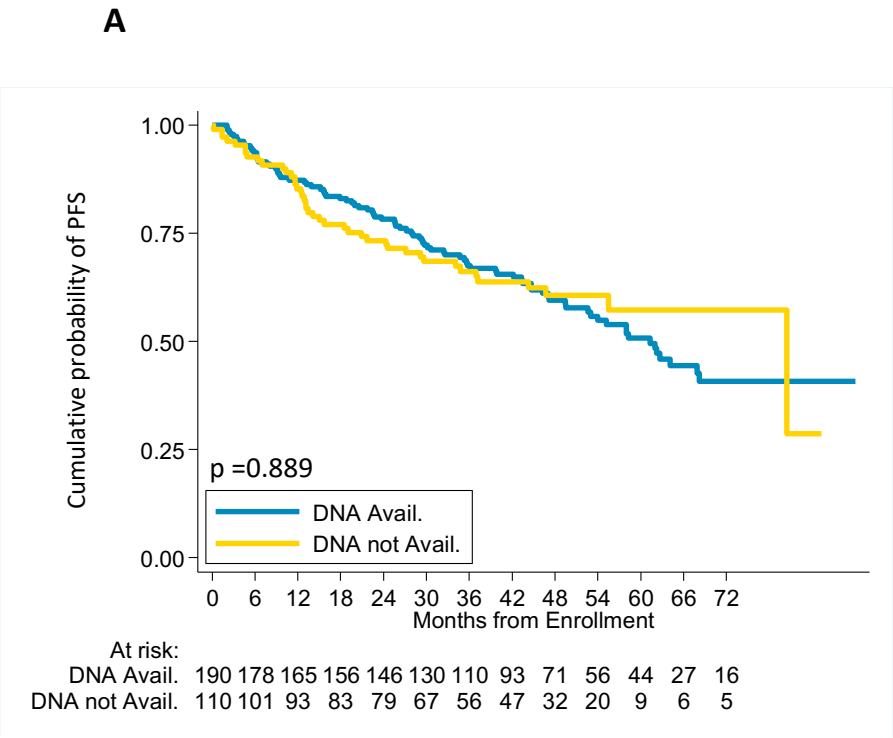
A
Cumulative probability of PFS
1.00
0.75
0.50
0.25
0.00
p =0.889
DNA Avail.
DNA not Avail.
0 6 12 18 24 30 36 42 48 54 60 66 72
Months from Enrollment
At risk:
DNA Avail. 190 178 165 156 146 130 110 93 71 56 44 27 16
DNA not Avail. 110 101 93 83 79 67 56 47 32 20 9 6 5

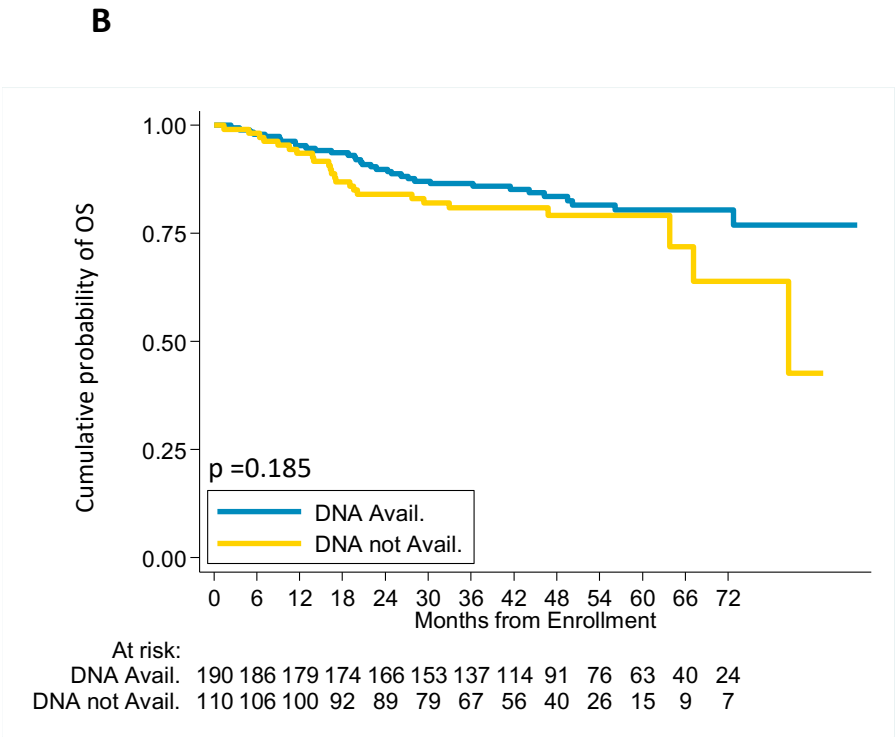
B
Cumulative probability of OS
1.00
0.75
0.50
0.25
0.00
p =0.185
DNA Avail.
DNA not Avail.
0 6 12 18 24 30 36 42 48 54 60 66 72
Months from Enrollment
At risk:
DNA Avail. 190 186 179 174 166 153 137 114 91 76 63 40 24
DNA not Avail. 110 106 100 92 89 79 67 56 40 26 15 9 7

Figure S1

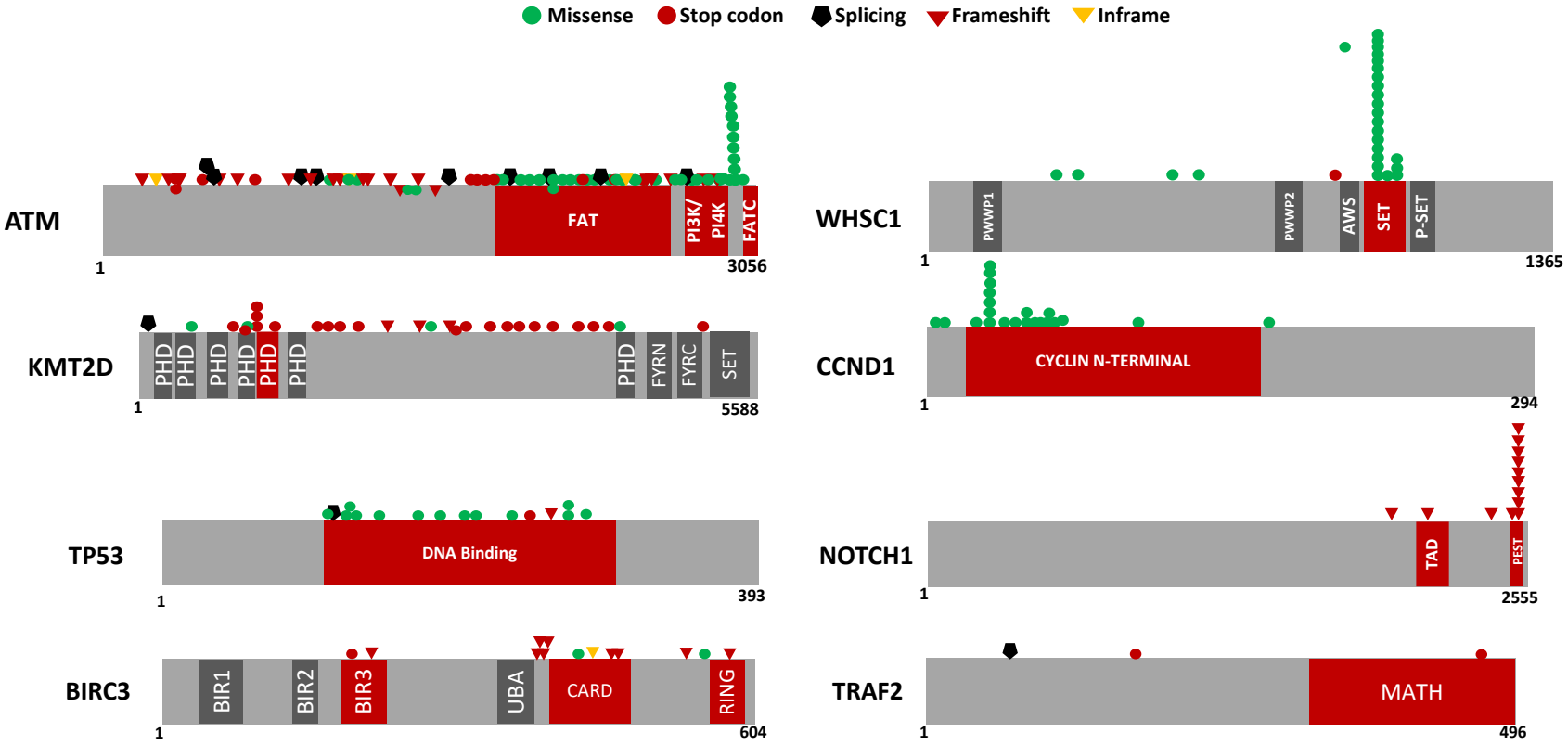
Missense
Stop codon
Splicing
Frameshift
Inframe
ATM
FAT
PI3K/ PI4K
FATC
1
3056
KMT2D
PHD
PHD
PHD
PHD
PHD
PHD
PHD
FYRN
FYRC
SET
1
5588
TP53
DNA Binding
1
393
BIRC3
BIR1
BIR2
BIR3
UBA
CARD
RING
1
604
WHSC1
PWWP1
PWWP2
AWS
SET
P-SET
1
1365
CCND1
CYCLIN N-TERMINAL
1
294
NOTCH1
TAD
PEST
1
2555
TRAF2
MATH
1
496

Figure S2

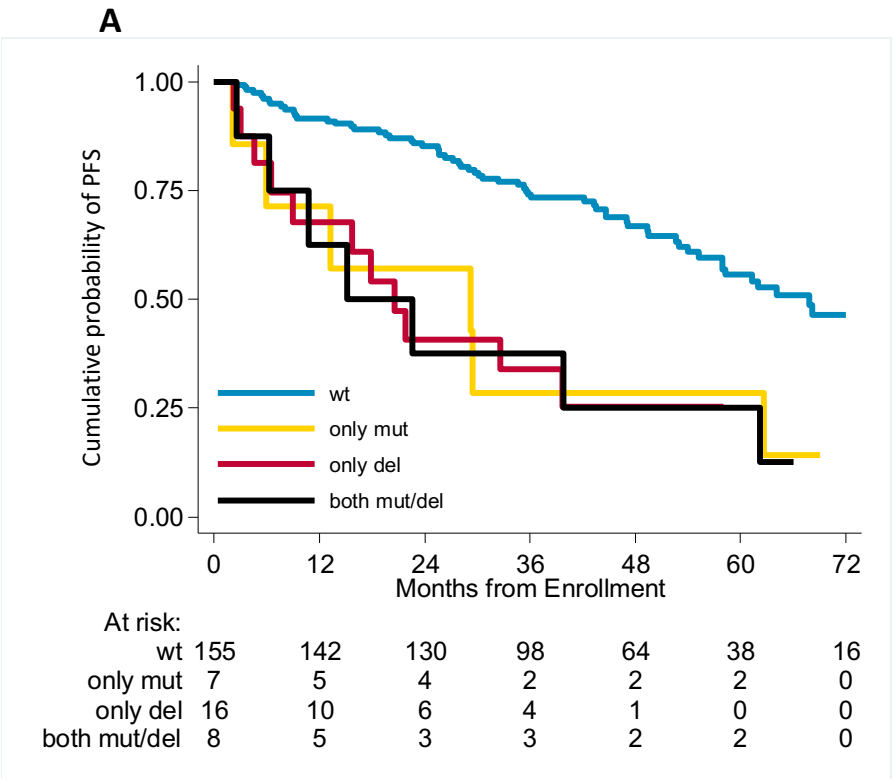
A
1.00
0.75
0.50
0.25
0.00
Cumulative probability of PFS
wt
only mut
only del
both mut/del
0
12
24
36
48
60
72
Months from Enrollment
At risk:
wt 155 142 130 98 64 38 16
only mut 7 5 4 2 2 2 0
only del 16 10 6 4 1 0 0
both mut/del 8 5 3 3 2 2 0

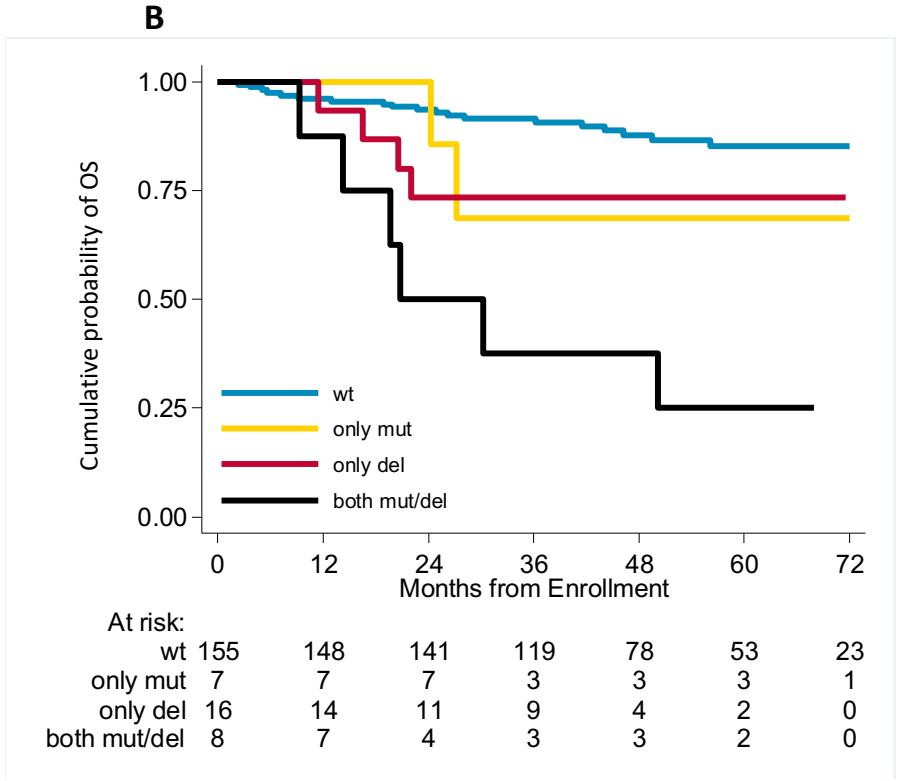
B
1.00
0.75
0.50
0.25
0.00
Cumulative probability of OS
wt
only mut
only del
both mut/del
0
12
24
36
48
60
72
Months from Enrollment
At risk:
wt 155 148 141 119 78 53 23
only mut 7 7 7 3 3 3 1
only del 16 14 11 9 4 2 0
both mut/del 8 7 4 3 3 2 0

Figure S3

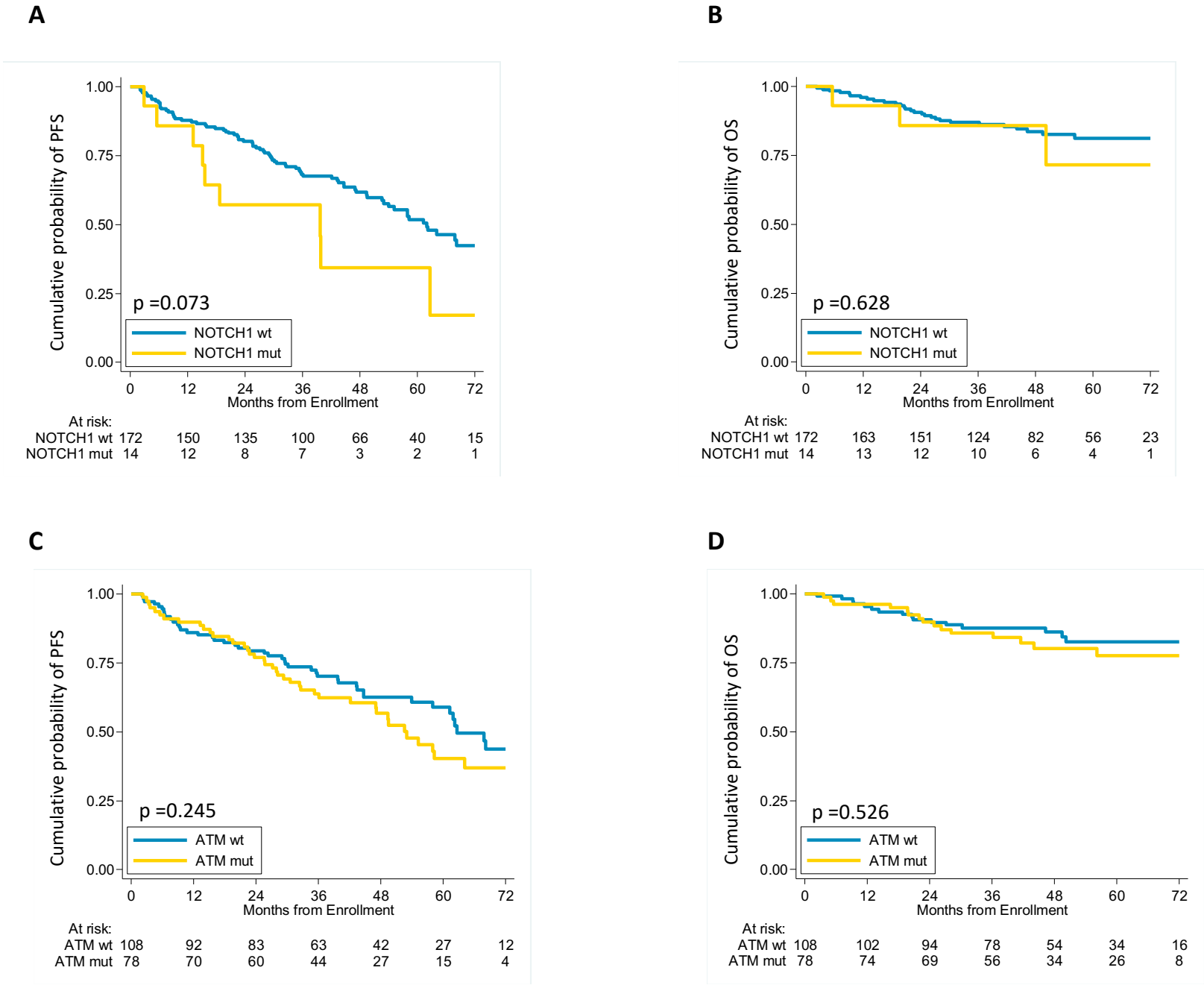
A
Cumulative probability of PFS
1.00
0.75
0.50
0.25
0.00
p =0.073
NOTCH1 wt
NOTCH1 mut
0 12 24 36 48 60 72
Months from Enrollment
At risk:
NOTCH1 wt 172 150 135 100 66 40 15
NOTCH1 mut 14 12 8 7 3 2 1
B
Cumulative probability of OS
1.00
0.75
0.50
0.25
0.00
p =0.628
NOTCH1 wt
NOTCH1 mut
0 12 24 36 48 60 72
Months from Enrollment
At risk:
NOTCH1 wt 172 163 151 124 82 56 23
NOTCH1 mut 14 13 12 10 6 4 1
C
Cumulative probability of PFS
1.00
0.75
0.50
0.25
0.00
p =0.245
ATM wt
ATM mut
0 12 24 36 48 60 72
Months from Enrollment
At risk:
ATM wt 108 92 83 63 42 27 12
ATM mut 78 70 60 44 27 15 4
D
Cumulative probability of OS
1.00
0.75
0.50
0.25
0.00
p =0.526
ATM wt
ATM mut
0 12 24 36 48 60 72
Months from Enrollment
At risk:
ATM wt 108 102 94 78 54 34 16
ATM mut 78 74 69 56 34 26 8

Figure S4

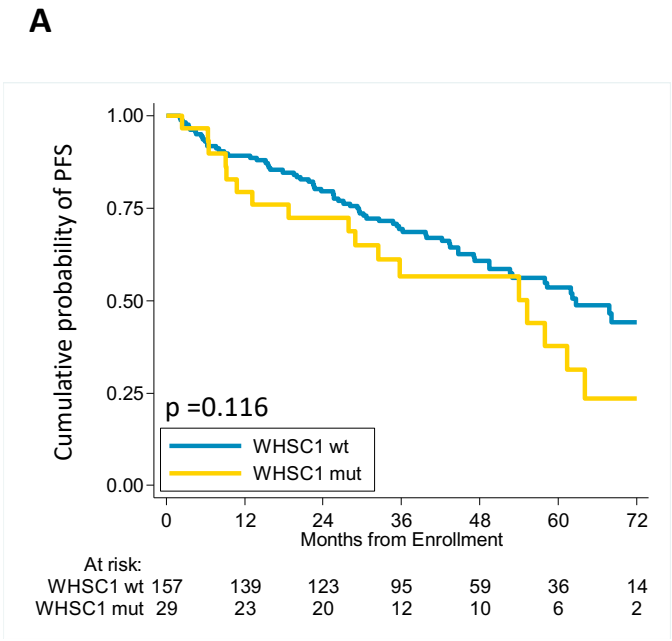
A
Cumulative probability of PFS
1.00
0.75
0.50
0.25
0.00
p =0.116
WHSC1 wt
WHSC1 mut
0
12
24
36
48
60
72
Months from Enrollment
At risk:
WHSC1 wt 157 139 123 95 59 36 14
WHSC1 mut 29 23 20 12 10 6 2

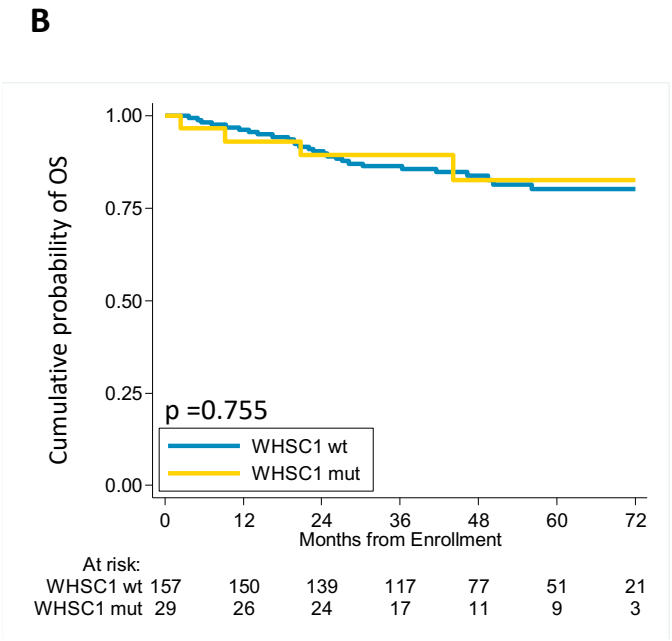
B
Cumulative probability of OS
1.00
0.75
0.50
0.25
0.00
p =0.755
WHSC1 wt
WHSC1 mut
0
12
24
36
48
60
72
Months from Enrollment
At risk:
WHSC1 wt 157 150 139 117 77 51 21
WHSC1 mut 29 26 24 17 11 9 3

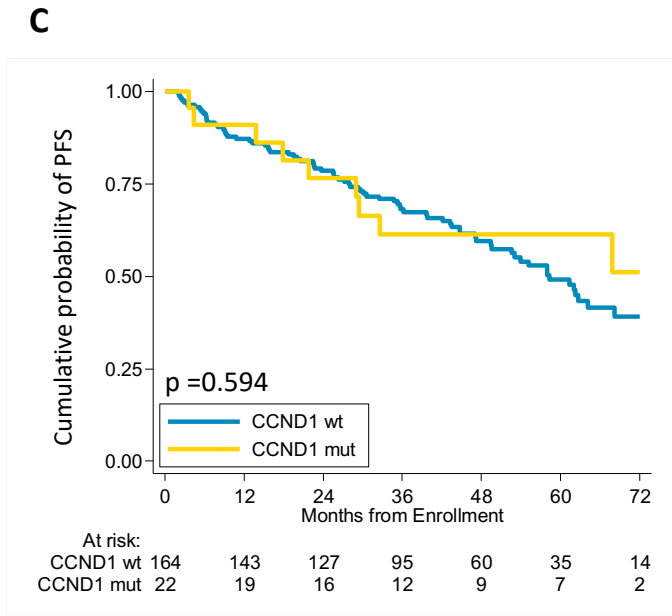
C
Cumulative probability of PFS
1.00
0.75
0.50
0.25
0.00
p =0.594
CCND1 wt
CCND1 mut
0
12
24
36
48
60
72
Months from Enrollment
At risk:
CCND1 wt 164 143 127 95 60 35 14
CCND1 mut 22 19 16 12 9 7 2

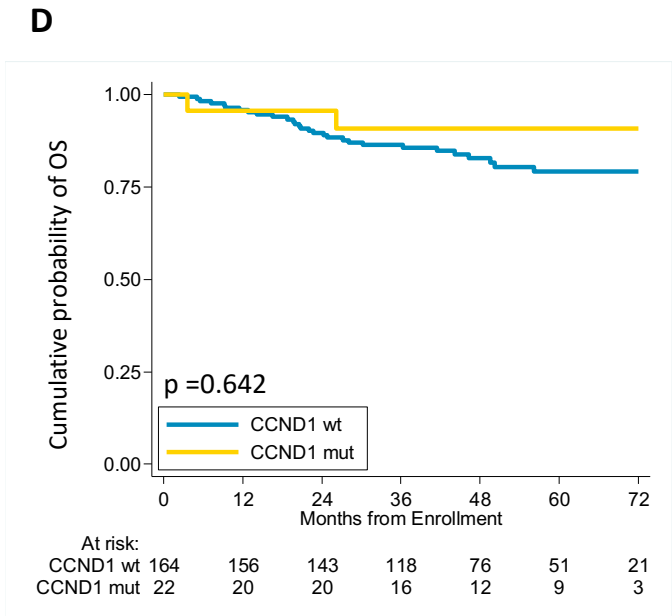
D
Cumulative probability of OS
1.00
0.75
0.50
0.25
0.00
p =0.642
CCND1 wt
CCND1 mut
0
12
24
36
48
60
72
Months from Enrollment
At risk:
CCND1 wt 164 156 143 118 76 51 21
CCND1 mut 22 20 20 16 12 9 3

Figure S5

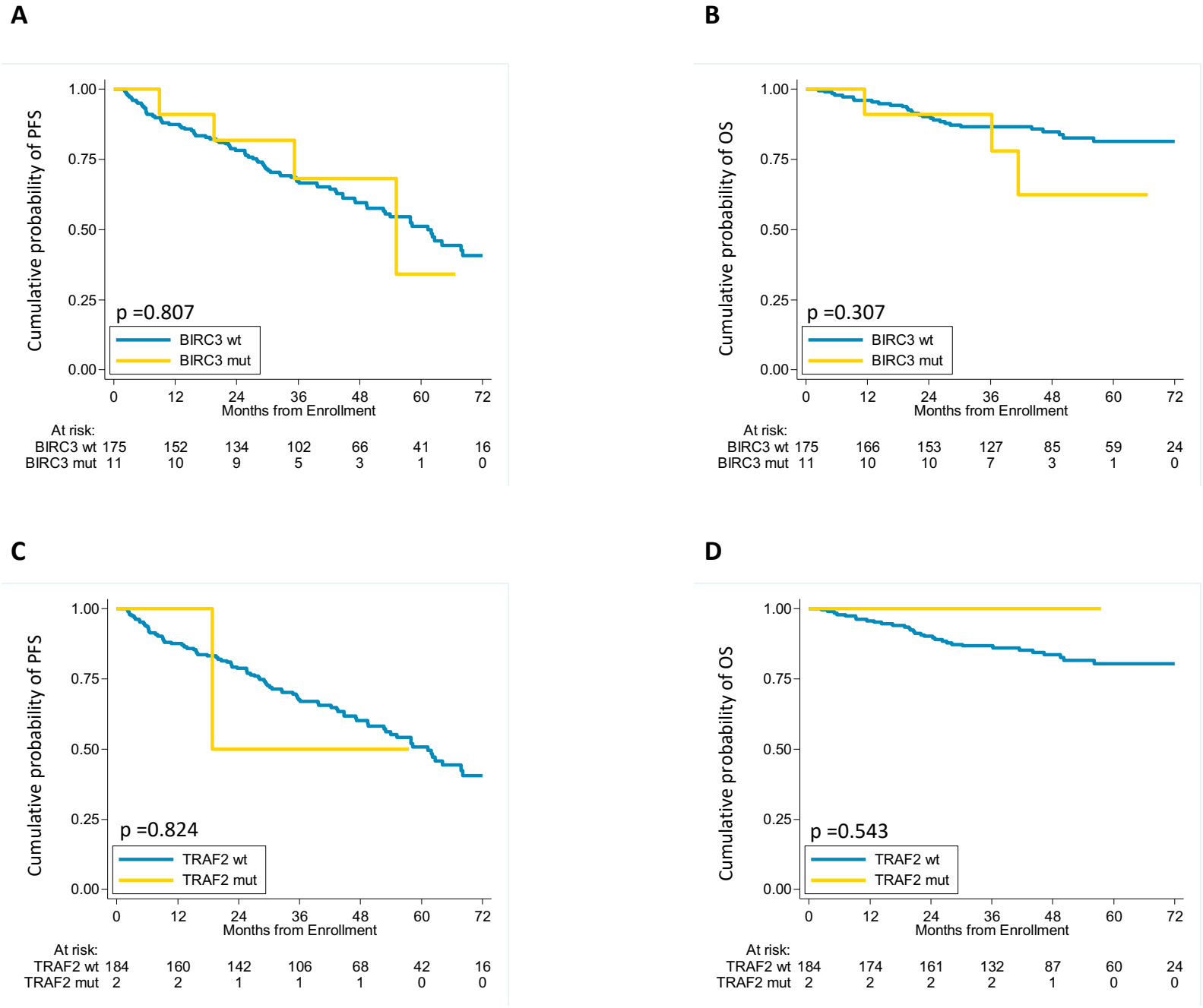
A
Cumulative probability of PFS
1.00
0.75
0.50
0.25
0.00
p =0.807
BIRC3 wt
BIRC3 mut
0 12 24 36 48 60 72
Months from Enrollment
At risk:
BIRC3 wt 175 152 134 102 66 41 16
BIRC3 mut 11 10 9 5 3 1 0
B
Cumulative probability of OS
1.00
0.75
0.50
0.25
0.00
p =0.307
BIRC3 wt
BIRC3 mut
0 12 24 36 48 60 72
Months from Enrollment
At risk:
BIRC3 wt 175 166 153 127 85 59 24
BIRC3 mut 11 10 10 7 3 1 0
C
Cumulative probability of PFS
1.00
0.75
0.50
0.25
0.00
p =0.824
TRAF2 wt
TRAF2 mut
0 12 24 36 48 60 72
Months from Enrollment
At risk:
TRAF2 wt 184 160 142 106 68 42 16
TRAF2 mut 2 2 1 1 1 0 0
D
Cumulative probability of OS
1.00
0.75
0.50
0.25
0.00
p =0.543
TRAF2 wt
TRAF2 mut
0 12 24 36 48 60 72
Months from Enrollment
At risk:
TRAF2 wt 184 174 161 132 87 60 24
TRAF2 mut 2 2 2 2 1 0 0

Figure S6

SUPPLEMENTARY TABLES EXCEL FILE ONLY

Table S1. Target region

Table S2. Somatic non-synonymous mutations discovered in the 186 cases of the molecular study

Table S3. Log-rank univariate analysis in terms of PFS and OS according to mutational status

Table S4. Clinical and biological baseline features of *KMT2D* and *TP53* disrupted patients

Table S5. MRD assessment after ASCT in *TP53* disrupted and in *KMT2D* mutated patients

Table S6. Multivariate analysis of *TP53* disruption and *KMT2D* mutations

SUPPLEMENTARY REFERENCES

1. Swerdlow SH, Campo E, Pileri SA, et al. The 2016 revision of the World Health Organization classification of lymphoid neoplasms. *Blood*. 2016;127(20):2375-2390.
2. Cortelazzo S, Martelli M, Ladetto M, et al. High Dose Sequential Chemotherapy with Rituximab and ASCT as First Line Therapy in Adult MCL Patients: Clinical and Molecular Response of the MCL0208 Trial, a FIL Study. *Haematologica.* 2015;100(s1): 3-4.
3. Beà S, Valdés-Mas R, Navarro A, et al. Landscape of somatic mutations and clonal evolution in mantle cell lymphoma. *Proc. Natl. Acad. Sci. U. S. A.* 2013;110(45):18250-18255.
4. Zhang J, Jima D, Moffitt AB, et al. The genomic landscape of mantle cell lymphoma is related to the epigenetically determined chromatin state of normal B cells. *Blood*. 2014;123(19):2988-2996.
5. Rahal R, Frick M, Romero R, et al. Pharmacological and genomic profiling identifies NF-κB-targeted treatment strategies for mantle cell lymphoma. *Nat. Med*. 2014;20(1):87-92.
6. Meissner B, Kridel R, Lim RS, et al. The E3 ubiquitin ligase UBR5 is recurrently mutated in mantle cell lymphoma. *Blood*. 2013;121(16):3161-3164.
7. Roccaro AM, Sacco A, Jimenez C, et al. C1013G/CXCR4 acts as a driver mutation of tumor progression and modulator of drug resistance in lymphoplasmacytic lymphoma. *Blood*. 2014;123(26):4120-4131.
8. Rinaldi A, Kwee I, Young KH, et al. Genome-wide high resolution DNA profiling of hairy cell leukaemia. *Br J Haematol*. 2013;162(4):566-569.
9. Kwee IW, Rinaldi A, de Campos CP, et al. Fast and Robust Segmentation of Copy Number Profiles Using Multi-Scale Edge Detection. *BioRxiv.* 2016. https://doi.org/10.1101/056705.

10. Voena C, Ladetto M, Astolfi M, et al. A novel nested-PCR strategy for the detection of rearranged immunoglobulin heavy-chain genes in B cell tumors. *Leukemia*. 1997;11(10):1793-1798.
11. Stamatopoulos K, Kosmas C, Belessi C, et al. Molecular analysis of bcl-1/IgH junctional sequences in mantle cell lymphoma: potential mechanism of the t(11;14) chromosomal translocation. *Br J Haematol*. 1999;105(1):190-197.
12. Pott C. Minimal residual disease detection in mantle cell lymphoma: technical aspects and clinical relevance. *Semin Hematol.* 2011;48(3):172-184.
13. Cheson BD, Pfistner B, Juweid ME, et al. Revised response criteria for malignant lymphoma. *J. Clin. Oncol.* 2007;25(5):579-586.